



## RESEARCH ARTICLE

10.1029/2022JG007245

# Metabolism Modeling in Rivers With Unsteady Flow Conditions and Transient Storage Zones

Devanshi Pathak<sup>1,2,3</sup>  and Benoît O. L. Demars<sup>4</sup> 

<sup>1</sup>UK Centre for Ecology and Hydrology, Wallingford, UK, <sup>2</sup>School of Geography and water@leeds, University of Leeds, Leeds, UK, <sup>3</sup>Now at Department of Aquatic Ecosystem Analysis and Management, Helmholtz Centre for Environmental Research-UFZ, Magdeburg, Germany, <sup>4</sup>Norwegian Institute for Water Research, Oslo, Norway

### Key Points:

- A metabolism model is developed by coupling an unsteady flow routing model with the two-station stream metabolism model
- The coupled modeling approach helps identify river reaches where transient storage needs to be accounted for when modeling metabolism
- The model allows metabolism estimation at the river network scale under changing environmental and management conditions

### Supporting Information:

Supporting Information may be found in the online version of this article.

### Correspondence to:

D. Pathak,  
[devanshi.pathak@ufz.de](mailto:devanshi.pathak@ufz.de)

### Citation:

Pathak, D., & Demars, B. O. L. (2023). Metabolism modeling in rivers with unsteady flow conditions and transient storage zones. *Journal of Geophysical Research: Biogeosciences*, 128, e2022JG007245. <https://doi.org/10.1029/2022JG007245>

Received 14 OCT 2022  
Accepted 7 MAR 2023

**Abstract** Whole-stream metabolism characterizes energy and carbon transformations, thus providing an estimate of the food base and CO<sub>2</sub> emission sources from streams and rivers. Metabolism models are generally implemented with a steady flow assumption that does not hold true for many systems with sub-daily flow variation, such as river sections downstream of dams. The steady flow assumption has confined metabolism estimation to a limited range of river environments, thus limiting our understanding about the influence of hydrology on biological production in rivers. Therefore, we couple a flow routing model with the two-station stream metabolism model to estimate metabolism under unsteady flow conditions in rivers. The model's applicability is further extended by including advection-dispersion processes to facilitate metabolism estimation in transient storage zones. Metabolism is estimated using two approaches: (a) an accounting approach similar to the conventional two-station method and (b) an inverse approach that estimates metabolism parameters using least squares minimization method. Both approaches are complementary since we use outputs of the accounting approach to constrain the inverse model parameters. The model application is demonstrated using a case study of an 11 km long stretch downstream of a hydropower plant in the River Otra in southern Norway. We present and test different formulations of the model to show that users can make an appropriate selection that best represents hydrology and solute transport mechanism in the river system of interest. The inclusion of unsteady flows and transient storage zones in the model unlocks new possibilities for studying metabolism controls in altered river ecosystems.

**Plain Language Summary** Whole-stream metabolism is not only an integrative measure of river ecosystem health, but also characterizes carbon transformations in freshwater systems. Therefore, it is important to accurately estimate metabolism in diverse river environments. To achieve this, we focus on addressing two limitations in the current metabolism models. First, we include the influence of sub-daily flow variation on metabolism. Such a variation is common below hydropower dams (also in irrigated agricultural watersheds, flashy systems, and rivers downstream of wastewater treatment plants) and has the potential to negatively impact metabolism. Second, we include the influence of transient storage zones on metabolism. These storage zones are like dead zones in rivers, where the movement of water and solutes may be slowed down compared to the rest of the flowing river. These zones may significantly influence metabolism because of the higher travel time of water and solute particles. Using a case study of the River Otra in southern Norway, we show that the model successfully includes the influence of aforementioned river environments in whole-stream metabolism estimation. The model provides opportunities to estimate metabolism in a wider range of river environments, which in turn will help reduce uncertainties in our global estimates of freshwater carbon fluxes.

## 1. Introduction

Biotic CO<sub>2</sub> emissions from rivers can be estimated through the metabolic balance of rivers, thus contributing to our understanding of the global carbon cycle (Battin et al., 2023; Hotchkiss et al., 2015; Raymond et al., 2013). Whole-stream metabolism characterizes carbon fixation and mineralization through gross primary production (GPP) and ecosystem respiration (ER) in streams and rivers. GPP and ER are integral measures of riverine biological processes (Bernhardt et al., 2018) and can serve as important indicators of whole-river health (Ferreira et al., 2020; Von Schiller et al., 2017; Young et al., 2008).

Ecologists have developed robust models for whole-stream metabolism estimation based on diel oxygen changes in open channels (Demars et al., 2015; Holtgrieve et al., 2016; Odum, 1956) including book-keeping methods

© 2023. The Authors.

This is an open access article under the terms of the [Creative Commons Attribution License](https://creativecommons.org/licenses/by/4.0/), which permits use, distribution and reproduction in any medium, provided the original work is properly cited.

with Monte Carlo simulation (Demars, 2019) and inverse models with Bayesian procedure (Appling, Hall, Yackulic, & Arroita, 2018; Hall et al., 2016; Holtgrieve et al., 2010). However, these models were developed for reach-scale estimation and for a limited range of river environments (Appling et al., 2018). For example, the open-channel metabolism models do not account for the influence of sub-daily flow variation and transient storage zones on dissolved oxygen (DO) variation at river-network scale despite these features being prevalent in many rivers due to flow regulation (Zimmerman et al., 2010) and channel hydromorphological characteristics (Kurz et al., 2017), respectively. Civil engineers have also produced water quality models for oxygen prediction to address river sanitation issues (Beck & Young, 1975; Streeter & Phelps, 1925). These models are applicable to entire river networks (Cox, 2003a, 2003b), whereas this is just emerging in the ecological literature (Pathak et al., 2022; Segatto et al., 2020, 2021). Therefore, we can integrate implementations from both these fields to build parsimonious models applicable at the river-network scale and to a wider range of river environments than those currently studied through open-channel metabolism models.

Quantification of transient storage in metabolism models may be crucial as these zones are potential hotspots of metabolism in rivers due to longer residence times (Argerich et al., 2011; Fellows et al., 2001; Mulholland et al., 2001). Transient storage zones are characterized by stagnant pockets of water due to presence of biofilms, dense patches of aquatic plants, hyporheos, or eddies of deep pools (Bencala & Walters, 1983; Bottacin-Busolin et al., 2009; Ensign & Doyle, 2005). Several models have been developed to simulate the impact of transient storage on solute transport in rivers such as the Transient Storage Model (Bencala & Walters, 1983; Manson et al., 2001; Runkel, 1998) and the Aggregated Dead Zone (ADZ) model (Beer & Young, 1983; Wallis et al., 1989). The proportion of transient storage and the exchange rate of water molecules between the main channel and the storage zone may change with flow (Manson et al., 2010; Wallis & Manson, 2018), but current models were designed to work under steady flows.

The assumption of steady flow conditions in metabolism models may not be valid in regulated rivers. Wide-spread flow regulation for reservoir operations in rivers around the world has altered the frequency and magnitude of sub-daily flow variation and consequently impacted healthy ecosystem functioning (Poff & Zimmerman, 2010). The timings and magnitude of flow releases determine trends in metabolism. Reduction in flow variability can elevate downstream metabolism (Aristi et al., 2014), whereas abrupt high-flow releases can reduce tailwater metabolism (Uehlinger et al., 2003). The studies analyzing flow regulation impacts on ecosystem metabolism have mainly looked at coarser temporal scale using Odum (1956)'s two-station method at a river-reach scale, where homogeneous hydraulic conditions are assumed over a period of day, that is, impact of average daily flow on average daily metabolism (e.g., Aristi et al., 2014; Chowanski et al., 2020; Uehlinger et al., 2003). However, metabolism models need to account for sub-daily flow variability, especially considering recent trends in the rapidly changing energy markets (e.g., switch to renewable energy) that may enhance the sub-daily variability in flow (hydropeaking) in tailwaters (Ashraf et al., 2018). To address these limitations, a river network model for stream metabolism requires the run of a flow routing model ahead of implementing the two-station method (Cimorelli et al., 2016; Payn et al., 2017; Whitehead et al., 1997). The prospect of simply adding water transient storage using advection-dispersion equations (Chapra & Runkel, 1999; Demars et al., 2015) to these more complicated models is daunting because many additional parameters would need to be estimated or well constrained to apply the models at river-network scale under varying flow conditions, as exemplified with nutrient cycling (Ye et al., 2012).

This study overcomes these limitations through development of a parsimonious model for Metabolism estimation in rivers with Unsteady Flow conditions and Transient storage zones (MUFT) that can be extended to a river-network scale. To demonstrate the model's development and implementation, we used a case study of the River Otra in southern Norway. The MUFT model was implemented along an 11 km river stretch downstream of a hydropower plant, where dam operations cause significant diel fluctuations in flow. To include the influence of diel flow variation in the MUFT model, we coupled a simple unsteady flow routing model adapted from the QUASAR (QUALity Simulation Along River systems) model (Whitehead et al., 1997) with a two-station stream metabolism model (Odum, 1956). The study stretch also demonstrates delayed oxygen transport compared to water velocity, which could be attributed either to the transient storage created from excessive plant growth in the river reach or to the dual flow regulation by dams at the upstream and downstream ends of the study stretch. To account for these probable mechanisms of oxygen transport, we tested two model formulations, (a) ADZ model that accounts for transient storage zones (Wallis et al., 1989) and (b) ADV (advection) model that accounts for dual flow regulation impact on oxygen transport (Beck & Young, 1975). In the MUFT model, these formulations

(ADV or ADZ) are coupled with the unsteady flow routing and the two-station stream metabolism models. Previously, studies have proposed modifications in the QUASAR flow routing model to simulate unsteady flows (Sincock & Lees, 2002) as well as proposed coupling of ADZ and original QUASAR (steady flow) models to simulate non-conservative solutes (Lees et al., 1998). The MUFT model combines these efforts by coupling the unsteady QUASAR model and the ADZ model to simulate non-conservative solutes.

In this study, we show metabolism estimation using both inverse and accounting (book-keeping) approaches in the MUFT model. While the accounting method is not predictive, it allows an independent estimation of the light parameters for GPP that are used to better constrain the inverse model and avoid issues of equifinality. The modeling approaches presented in this study not only provide theoretical benefits for studying the impact of transient storage zones and unsteady flows on metabolism dynamics, but also promote practical applications for the management of tailwater river ecosystems.

## 2. Theory

We first selected a flow routing model to simulate discharge downstream of a hydropower plant, with upstream flow boundary conditions (from e.g., gauging station, rainfall-runoff simulations) as model input. We present the flow model equations in this section, but any flow routing model of user's preference can be used. Further, we present associated metabolic models of DO concentrations under unsteady flow conditions with increasing complexity. In the next section, we show how to apply these models to a case study.

### 2.1. Flow Routing Model

To simulate unsteady flows in the MUFT approach, we adapted the flow routing model proposed by Sincock and Lees (2002), who based their approach on the QUASAR model (Whitehead et al., 1997) originally designed for slowly time-varying flows (quasi-steady-state). Because of the steady flow assumption, the original QUASAR model assumes the flow and solute travel times to be equal. However, under unsteady flow conditions, the travel time of flood wave can be expressed in terms of kinematic wave velocity (celerity), which is higher than the mean flow velocity (Sincock et al., 2003) and consequently, solute velocity. The ratio  $m$  of the average celerity ( $c$ ,  $m\ s^{-1}$ ) to the average flow velocity ( $u$ ,  $m\ s^{-1}$ ) is expressed following Sincock et al. (2003),

$$m = \frac{c}{u} = \frac{dQ/dA}{Q/A} \quad (1)$$

where  $Q$  is discharge ( $m^3\ s^{-1}$ ),  $A$  is the cross-section area of flow and  $m$  may be approximated as 5/3 from the Manning friction law (Chapra, 2008).

The celerity ( $c$ ,  $m\ s^{-1}$ ) of the flood wave for a reach of length  $L$  (m) is,

$$c = \frac{L}{T_{flow}} \quad (2)$$

where  $T_{flow}$  represents the travel time of the flood wave (s).

It is assumed that  $T_{flow}$  may be partitioned into dispersion ( $T_{fladz}$ ) and advection ( $\tau_{fl}$ ) terms using a fraction of retention  $F_r$ ,

$$T_{fladz} = F_r \times T_{flow} \quad (3)$$

$$\tau_{fl} = (1 - F_r) \times T_{flow} \quad (4)$$

The flow routing model includes a simple mass-balance of incoming and outgoing flows and assumes fixed channel width with rectangular cross-section. Lateral groundwater inflows and discharge from small tributaries were assumed to be negligible within reaches. In a river network, the flow of major tributaries may be inserted at the upstream edge of a reach. River reaches may be represented as a series of nonlinear reservoirs. The flow model simulates water transport through a series of  $n$  nonlinear reservoirs followed by a time lag parameter ( $\tau_{fl}$ , s) that lags the routed hydrograph without attenuation (Figure 1a). The changes in flow are represented as follows,

$$\frac{dQ_t}{dt} = \frac{Q_{i,t-\tau_{fl}} - Q_t}{F_r T_{flow}} \quad (5)$$

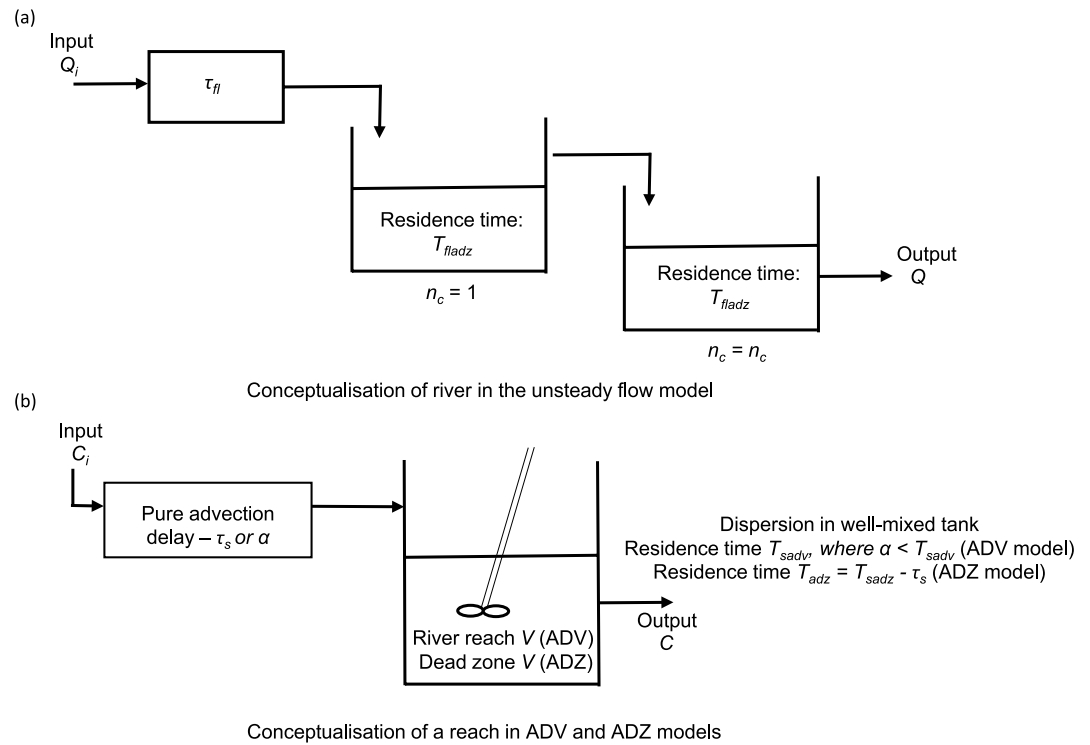


**Figure 1.** Conceptualization of river reaches in the (a) unsteady flow model adapted from Sincock and Lees (2002) and (b) ADV and ADZ models adapted from Lees et al. (2000) for conservative solute  $C$ .  $Q_i$ , Input flow,  $Q$ , output flow,  $\tau_{fl}$ , advection fraction of flood wave travel time,  $T_{fladz}$ , dispersion fraction of flood wave travel time,  $n_c$ , number of continuous stirred-tank reactors,  $C_i$ , input dissolved oxygen concentration,  $C$ , output dissolved oxygen concentration,  $\alpha$  and  $\tau_s$ , advection delay in ADV and ADZ models,  $T_{sadv}$ , total solute travel time in the ADV model,  $T_{adz}$ , dead zone residence time in the ADZ model,  $T_{sadz}$ , total solute travel time in the ADZ model.

where  $Q_t$  is the flow leaving the reach at time-step  $t$ ,  $Q_{i,t}$  is the flow coming into the reach at time-step  $t$  ( $i$  represents input). Equation 5 accounts for the travel time ( $T_{flow}$ ) derived from celerity (Equation 2) as opposed to the travel time derived from mean flow velocity as is commonly done in original QUASAR model applications.

## 2.2. Metabolic Model in a Well-Mixed Reach Under Unsteady Flow Conditions

We developed the metabolic model of DO dynamics (Equation 6) by combining two approaches, (a) the conservative solute transport model proposed by Whitehead et al. (1997) to simulate DO transport with unsteady flows and (b) the two-station stream metabolism method proposed by Odum (1956) to simulate in-stream DO sources and sinks from metabolism and air-water gas exchange processes. The detailed proofs of both models were given in the original publications. Note that Equation 6 does not account for water transient storage.

$$\frac{dC_t}{dt} = \frac{Q_{i,t}}{(Q_t \times T_u)} (C_{i,t} - C_t) + \frac{1}{z_t} (P_{GPP,t} - R_{ER,t}) + k(C_{s,t} - C_t) \quad (6)$$

where  $C_{i,t}$  is the incoming DO in the reach at time-step  $t$  ( $\text{mg O}_2 \text{ L}^{-1}$  equivalent to  $\text{g O}_2 \text{ m}^{-3}$ ),  $C_t$  is the DO leaving the reach at time-step  $t$  ( $\text{mg O}_2 \text{ L}^{-1}$ ),  $z_t$  is the average stream water depth (m),  $P_{GPP}$  is the GPP ( $\text{g O}_2 \text{ m}^{-2} \text{ min}^{-1}$ ),  $R_{ER}$  is the ER ( $\text{g O}_2 \text{ m}^{-2} \text{ min}^{-1}$ ),  $k$  is the gas exchange coefficient ( $\text{min}^{-1}$ ) and  $C_s$  is the expected oxygen solubility ( $\text{mg O}_2 \text{ L}^{-1}$ ).  $T_u$  (min) represents the mean flow travel time, which is equal to the solute travel time for a well-mixed reach.

## 2.3. Metabolic Model With Pure Advection and a Well-Mixed Reach Under Unsteady Flows (ADV Model)

In long reaches where solute transport is dominated by advective transport as opposed to dispersion, it may be necessary to explicitly take into account pure advection as shown in Equation 7 (Beck & Young, 1975;

Odum, 1956). The ADV formulation accounts for the effect of dual water regulation by dams at upstream and downstream ends of the study reach. The dual water regulation results in apparent faster water velocity compared to the solute velocity due to the early release of water by the downstream dam before the water from the upstream dam reaches the downstream dam.

$$\frac{dC_t}{dt} = \frac{Q_{i,t-\alpha}}{(Q_t \times T_{sadv})} (C_{i,t-\alpha} - C_t) + \frac{1}{z_t} (P_{GPP,t} - R_{ER,t}) + k(C_{s,t} - C_t) \quad (7)$$

$$\alpha = F_{adv} \times T_{sadv} \quad (8)$$

where  $F_{adv}$  is the advection delay coefficient. The addition of pure advection  $\alpha$  in the first term of the equation allows to have the two DO concentration curves in phase without modifying their shape (simple time translation), with  $\alpha \leq T_{sadv}$  (Beck & Young, 1975). Note that  $T_{sadv}$  is equivalent to  $T_u$  for the ADV model.

#### 2.4. Metabolic Model With Pure Advection and Transient Storage (Dispersion) Under Unsteady Flows (ADZ Model)

The influence of transient storage in the metabolic model is included using the ADZ concept (Beer & Young, 1983; Wallis et al., 1989) as proposed by Sincock and Lees (2002), who coupled the unsteady QUASAR flow model with the ADZ model for a conservative solute. ADZ model was selected for its simplicity and its conceptual similarity to the unsteady QUASAR flow model (Figure 1). The original QUASAR model assumes the river reach to be a perfectly mixed system. ADZ model conceptualizes the river reach as an imperfectly mixed system, where the solute is subjected to pure advection followed by dispersion in a lumped active mixing zone (Beer & Young, 1983; Lees et al., 2000; Wallis et al., 1989). The metabolic model becomes:

$$\frac{dC_t}{dt} = \frac{Q_{i,t-\tau_s}}{(Q_t \times T_{adz})} (C_{i,t-\tau_s} - C_t) + \frac{1}{z_t} (P_{GPP,t} - R_{ER,t}) + k(C_{s,t} - C_t) \quad (9)$$

The ADZ model partitions the overall solute travel time  $T_{sadv}$  into dead-zone residence time  $T_{adz}$  and advection lag  $\tau_s$ , equivalent to partitioning total reach volume into the volume of water transient storage and main channel.

$$T_{adz} = T_{sadv} - \tau_s \quad (10)$$

For reaches affected by transient storage, the effective solute transport velocity ( $u_s$ ) is lower than the mean flow velocity ( $u$ ) due to solute retention in the storage zone. The relationship between these velocities can be described using a solute-lag coefficient  $\beta$  (Lees & Camacho, 2000) as follows,

$$u_s = \frac{u}{1 + \beta} \quad (11)$$

Considering Equations 1, 2, and 11, travel time and advection lag for a solute in the ADZ model can be described in terms of flow parameters (Sincock, 2002),

$$T_{sadv} = m(1 + \beta)T_{flow} \quad (12)$$

$$\tau_s = m(1 + \beta)\tau_{fl} \quad (13)$$

#### 2.5. Modified Two-Station Model for the Accounting Method

Equation 9 can be simplified to derive net ecosystem production ( $P_{NEP} = P_{GPP} - R_{ER}$ ) using Euler finite-difference approach, which gives the two-station accounting approach under varying discharge,

$$P_{NEP,t} = \left( \frac{C_{i,t+\Delta t} - C_t}{\Delta t} - \frac{Q_{i,t-\tau_s}}{(Q_t \times T_{adz})} (C_{i,t-\tau_s} - C_t) - k(C_{s,t} - C_t) \right) z_t \quad (14)$$

Note that Equation 14 can easily be adjusted for the other metabolic models presented above (Equations 6 and 7). This approach allows to estimate average  $R_{ER}$  during the dark hours (photosynthetically active radiation [PAR] < 1  $\mu\text{mol-photon m}^{-2} \text{s}^{-1}$ ) and deduce  $P_{GPP,t}$  by difference ( $P_{NEP,t} - R_{ER,t}$ ) during the light hours assuming constant  $R_{ER}$  throughout the day (see Demars et al., 2015). Daily GPP ( $P_{GPP}$ ) is simply the sum of  $P_{GPP,t}$  throughout a day,

$$P_{GPP} = \frac{\int_{t_0}^{t_{end}} P_{GPP,t} dt}{1 \text{ day}} \quad (15)$$

## 2.6. Photosynthesis-Light Relationship

The accounting method has the advantage, over the inverse modeling approach, of deriving instantaneous and daily GPP without making any assumption on the photosynthesis-light relationship. The most appropriate link function may thus be selected by plotting  $P_{GPP,t}$  as a function of  $PAR_t$ . The function is substituted to  $P_{GPP,t}$  in the metabolic models (Equations 6, 7, or 9). The parameters of the link function may be used as constants or enabled to constrain the priors (through their uncertainties) in the inverse model, thus reducing issues of equifinality. Here, instantaneous GPP ( $P_{GPP}$ ) was modeled as a function of PAR with a Michaelis-Menten type equation to include the light-saturation effect on photosynthesis (Demars et al., 2011),

$$P_{GPP,t} = \frac{P_{GPPmax} \times E_{PAR,t}}{k_{PAR} + E_{PAR,t}} \quad (16)$$

where  $E_{PAR,t}$  is the PAR ( $\mu\text{mol-photon m}^{-2} \text{ s}^{-1}$ ) at time-step  $t$ ,  $P_{GPPmax}$  is the maximum GPP ( $\text{g O}_2 \text{ m}^{-2} \text{ min}^{-1}$ ) and  $k_{PAR}$  is the PAR at which half the  $P_{GPPmax}$  is attained ( $\mu\text{mol-photon m}^{-2} \text{ s}^{-1}$ ).

$P_{GPPmax}$  and  $k_{PAR}$  in the inverse model were estimated using a least squares minimization algorithm. It is implicitly assumed that light conditions are spatially uniform along the modeled channel length and PAR only varies with time.

## 2.7. Dissolved Oxygen Saturated Concentration

The expected oxygen solubility ( $C_s$ ,  $\text{mg L}^{-1}$ ) was estimated from Standing Committee of Analysts (1989) as follows,

$$C_s = \frac{C_{atm}(P - V_p)}{101.325 - V_p} \quad (17)$$

where  $C_{atm}$  is the oxygen solubility under normal atmospheric pressure ( $\text{mg L}^{-1}$ ),  $P$  is the observed atmospheric pressure (kPa) and  $V_p$  is the saturation vapor pressure of water (kPa).  $C_{atm}$  and  $V_p$  were estimated as a function of water temperature  $T$  (range of application  $0^\circ\text{C}$ – $50^\circ\text{C}$ , Demars et al., 2015),

$$C_{atm} = -0.00005858T^3 + 0.007195T^2 - 0.39509T + 14.586 \quad (18)$$

$$V_p = 0.0000802T^3 - 0.000717T^2 + 0.0717T + 0.539 \quad (19)$$

## 3. Case Study

### 3.1. Study Area

The River Otra flows through forests and alpine uplands in the valley of Setesdal and is the largest river in southern Norway. The river drains a catchment area of  $4,000 \text{ km}^2$  and runs for about 240 km until it meets the North Sea at Kristiansand (Wright et al., 2017). The river is extensively used for hydropower production (about 4 TWh per year) through the construction of dams and water transfers, with Brokke being the largest hydropower station in the valley (Rørslett, 1988; Wright et al., 2017).

We applied the models within a 10,780 m long river section located downstream of the Brokke hydropower plant (Figure 2). This section drains about  $1,900 \text{ km}^2$  (Wright et al., 2017). The river stretch can be considered an artificial system with its flow and water level controlled by Brokke hydropower plant at the upstream end and Hekni dam at the downstream end. The oscillating demands on energy production can cause flow to vary from  $\sim 20$  to  $80 \text{ m}^3 \text{ s}^{-1}$  within 24 hr under low summer flows (Figure 4a). The hydropower plant effluent can also release water highly supersaturated in dissolved gases depending on water intakes (streams vs. reservoirs) independently of discharge (Pulg et al., 2016). No such supersaturation events were observed during the short-term

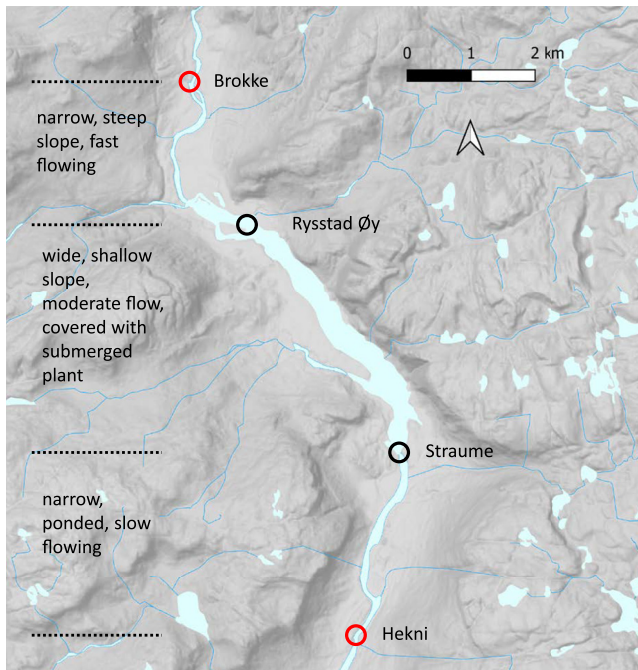


**Figure 2.** Study stretch in the River Otra spanning from Brokke to Hekni. Monitoring locations of river flow (red circles) and dissolved oxygen (black circles) are marked on the map.

study period here (Demars et al., 2021). In addition to the controlled flow, the river reach also shows profuse growth of the aquatic plant *Juncus bulbosus*, which may create a significant amount of water transient storage, delaying solute transport time relative to the velocity of water (Ensign & Doyle, 2005; Kurz et al., 2017).

### 3.2. Sensor Deployment and Bathymetry

DO and water temperature were monitored using O<sub>2</sub> and temperature sensors (miniDOT PME) at site 2 (Figure 2). A monitoring station was also installed at site 3 to monitor DO and water temperature (Xylem - Andeera optode 4831), PAR (LICOR Quantum LI190R-L), air temperature and atmospheric pressure (Barometer RM Young 061302V) using a Campbell data logger (CR1000X). Data from the monitoring station were transferred daily through a Campbell Scientific 4G modem CELL215. Data were logged at 5 min time intervals from 4th (10:00 a.m.) to 8th (15:35) August 2019. The sensor at site 2 was installed vertically facing down in the main current at middepth, tied to a post. The sensor at site 3 was inserted into a plastic pipe fixed on Straume Bridge, and protruded in the main current. The oxygen sensors were cross calibrated in 100% air saturated water in a bucket before and after deployment and small corrections (<3% DO saturation) were applied, as previously reported (Demars, 2019).

Total dissolved gas (TDG) was monitored at sites 1–4 every 30 min at infrequent intervals during a 5 yr period (2012–2017) with Total Gas Analyzers 3.0 (Fisch-und Wassertechnik (Pulg et al., 2016) based on the Weiss-saturometer principle (Weiss, 1970). The saturation is measured as the percent dissolved

air in the water relative to expectation from ambient air pressure. The satumeter has an accuracy of  $\pm 10$  hPa, which is approximately  $\pm 1\%$  TDG.

Several thousands of georeferenced water depth points were taken throughout the reach with a measuring stick north of Straume and sonar (Lowrance) in the downstream part to Hekni (Figure S1 in Supporting Information S1), and cross-calibrated with discharge. Changes in water depth were determined from absolute pressure difference (see Moe & Demars, 2017) between atmospheric pressure and submersible pressure sensors inserted into a perforated plastic tube at sites 1–4 recording at 30 min time intervals (Onset HOBO data loggers U20L-04, accuracy equivalent to 4 mm for water level).

### 3.3. Flow-Velocity

Hourly flow data at Brokke (hydropower plant effluent and river) and Hekni sites were obtained for a duration of 8 days (3 August 2019 to 10 August 2019) from the hydropower company. Flow observations were not available at Rysstad Øy and Straume, where metabolism is estimated. Flood wave travel times at these sites were derived from solute travel time using the travel time relationships proposed by Sincock et al. (2003). We used these travel time relationships to back-calculate solute and flow travel time parameters from velocity estimates (Table 1). Velocity estimates in the river reaches were derived using two approaches.

Average velocities for the first section (sites 1–2: steep, shallow, fast flowing, cobble bed) were determined using Manning's equation:  $u_s = (1/n_m)A/P_m^{2/3}S_c^{1/2}$ , where  $n_m$  is the Manning roughness coefficient (0.04, cobble bed),  $A$  is the cross-sectional area of the river channel (m<sup>2</sup>),  $P_m$  is the wetted perimeter of the river channel (m) and  $S_c$  is the channel slope (0.0016 m/m).  $A$  and  $P_m$  were calculated using changes in water depth. This method could not be applied further downstream due to partial control on water level by Hekni dam.

Average velocities for the second section (sites 2–3: very wide, gentle slope, sandy bed) and the third section (sites 3–4: narrow, water level controlled by Hekni dam) were estimated from section length ( $L$ ) and mean travel time ( $T_s$ ) of large peaks in TDG, where  $u_s = L/T_s$ . We used cross-correlation function in R (Venables & Ripley, 2002) to identify average travel time lags ( $h$ ) between TDG time-series across the sites. Large TDG super-saturation

**Table 1**

*Velocity and Travel Time Formulations in the ADV and ADZ Models for the River Otra Back-Calculated Based on the Travel Time Relationships Proposed by Sincock et al. (2003)<sup>a</sup>*

	ADV model	ADZ model
Solute velocity	$u_s = b' \times Q^{c'}$	$u_s = b' \times Q^{c'}$
Solute-lag coefficient	$\beta = 0$	$\beta = 1.55$ (see Text S2 in Supporting Information S1)
Mean flow velocity	$u_{adv} = u_s$	$u_{adz} = (1 + \beta) \times u_s$
Celerity	$c_{adv} = m \times u_{adv}$	$c_{adz} = m \times u_{adz}$
Water residence time in CSTR	$T_{uadv} = L/u_{adv}$	$T_{uadz} = L/u_{adz}$
Total solute travel time	$T_{sadv} = T_{uadv}$	$T_{sadz} = L/u_s$
Advection delay	$\alpha = F_{adv} \times T_{sadv}$	$\tau_s = T_{sadz} - T_{uadz}$
Dead zone residence time		$T_{adz} = T_{uadz}$

<sup>a</sup>CSTR, continuous stirred-tank reactor;  $b'$  and  $c'$ , flow-velocity constants;  $Q$ , discharge;  $\beta$ , solute-lag coefficient;  $u_{adv}$  and  $u_{adz}$ , mean flow velocity (ADV, ADZ);  $u_s$ , solute velocity;  $c_{adv}$  and  $c_{adz}$ , celerity (ADV, ADZ);  $m$ , constant;  $T_{uadv}$  and  $T_{uadz}$ , water residence time in CSTR (ADV, ADZ);  $L$ , reach length;  $T_{sadv}$  and  $T_{sadz}$ , total solute travel time (ADV, ADZ);  $\alpha$  and  $\tau_s$ , advection delay (ADV, ADZ);  $F_{adv}$ , advection delay coefficient;  $T_{adz}$ , dead zone residence time.

events (threshold >130% at Brokke) with time lag correlation coefficient >0.4 were selected for the estimation of velocity. These velocities were plotted against discharge at Hekni (averaged for corresponding event duration) to establish flow-velocity relationship for each reach. TDG travel times ranged between 2–12 and 7–13 hr in the second (sites 2–3) and third sections (sites 3–4), respectively. This method could not be applied in the first section as the temporal resolution of the TDG data was too coarse relative to the mean travel time (<1 hr).

We established relationships between flow and TDG velocity as  $u_s = b'Q^{c'}$  for three discernible sections. Ideally, a conservative solute should be used to estimate flow-velocity parameters ( $b'$ ,  $c'$ ). While TDG is not a conservative tracer, the selection of the largest peaks to differentiate from noise and the very low gas exchange rate in these sections gave a similar result to a continuous addition of lime under high flow conditions (about  $102 \text{ m}^3 \text{ s}^{-1}$ ) monitored with electric conductivity sensors deployed at Straume (site 3) and Hekni (site 4). Power regressions between the velocities of TDG waves and corresponding mean flows at Hekni provided values of constants  $b'$  and  $c'$  for the second ( $R^2 = 0.78$ ) and third sections ( $R^2 = 0.56$ ) (Figure S2 and Table S1 in Supporting Information S1). Water traveled fastest in the first section (Brokke-Rysstad Øy) with a mean velocity of  $0.73 \text{ m s}^{-1}$ , slowest ( $0.14 \text{ m s}^{-1}$ ) in the widest section with high plant growth (Rysstad Øy-Straume) and slow-flowing in the narrower and deeper third section ( $0.27 \text{ m s}^{-1}$ ) for a  $50 \text{ m}^3 \text{ s}^{-1}$  discharge.

### 3.4. Gas Exchange Rate

The gas transfer velocity ( $kz$ ) of  $\text{CO}_2$  was estimated as the flux of  $\text{CO}_2$  ( $F_{\text{CO}_2}$ ,  $\text{mmol m}^{-2} \text{ h}^{-1}$ ) determined using floating chambers equipped with infra-red gas analyzers (following Bastviken et al., 2015) relative to the  $\text{CO}_2$  saturation deficit as follows ( $C_s - C$ ,  $\text{mmol m}^{-3}$ ),

$$kz = \frac{F_{\text{CO}_2}}{C_s - C} \quad (20)$$

More specifically,  $\text{CO}_2$  efflux (or influx) were estimated in 33 half-hour runs, from the average of three chambers for each run drifting freely at the water surface and logging at 30 s time intervals. The runs were conducted between March 2020 and August 2020 under varying temperature, discharge, and depth. The calculations of  $\text{CO}_2$  flux for individual chambers followed Martinsen et al. (2018). Water samples were collected at the beginning and end of each run in 120 mL glass bottles to determine the  $\text{CO}_2$  saturation deficit. Water bottles were filled to the rim and capped underwater, then crimped. Mercuric chloride ( $\text{HgCl}_2$ ) was immediately added to stop biological processes (100  $\mu\text{L}$  of half saturated solution per 120 mL bottle). The samples were kept cool ( $+4^\circ\text{C}$ ) and in the dark until the day of gas analysis. The samples were warmed and weighed at room temperature, a 30 mL helium headspace was created, the samples were weighed again (to determine the volume of water removed from the bottle), and shaken gently horizontally for at least an hour. The headspace was analyzed by gas chromatography

and concentrations were calculated following Yang et al. (2015). It was checked that the addition of  $\text{HgCl}_2$  did not affect the determination of  $\text{CO}_2$  (Borges et al., 2019; Koschorreck et al., 2021).

The specific flux  $F_{\text{CO}_2}$  was not related to water temperature, discharge, depth, or velocity. Thus  $kz = 0.022 \pm 0.004 \text{ m hr}^{-1}$  was estimated as the slope of the regression line between specific  $\text{CO}_2$  flux and  $\text{CO}_2$  saturation deficit (Figure S3 in Supporting Information S1). In theory, the regression line should go through the origin, but the uncertainties were reasonable given the modest range of dissolved  $\text{CO}_2$  saturation (70%–267%). Thus, knowing the average depth ( $z = 1.82 \text{ m}$ ) during the chamber runs, the gas exchange coefficient was calculated for  $\text{CO}_2$  as  $k_{\text{CO}_2} = 0.012 \pm 0.002 \text{ hr}^{-1}$ .

Finally, the oxygen gas exchange coefficient  $k$  was simply calculated from  $k = k_{\text{CO}_2}/0.81$  (Demars, 2019), where the constant 0.81 accounts for differences in the rates of  $\text{CO}_2$  and  $\text{O}_2$  diffusion in water independently of temperature (Davidson, 1957). The estimate of  $k$  ( $0.35 \pm 0.07 \text{ days}^{-1}$ ) indicated low gas exchange, comparable to other rivers with similar depth-velocity ( $<2 \text{ days}^{-1}$ , Palumbo & Brown, 2014).  $k$  was used as a constant in the metabolism models (in Equations 6, 7, and 9) to simulate reaeration flux.

### 3.5. Model Application and Parameter Estimation

We developed the model code in Python (3.6.3) and it is available on Zenodo repository (Pathak, 2022). Flow and solute dynamics in the river were described using ordinary differential equations, and solved through an accounting method using finite difference approximation and inverse modeling using `odeint()` function from the Scipy package (v1.5.0) in python. The `odeint()` function solves ordinary differential equations using `lsoda` solver from the FORTRAN library `odepack`.

The boundaries of the river network for model implementation were decided based on data availability. The modeling approach presented here requires observations at minimum of two sites in the river, one for input and one for parameter calibration. The flow routing model was first implemented at 5 min time-steps for the river stretch between Brokke and Hekni since flow hydrographs were available at these two sites. Flows at Rysstad Øy and Straume were then simulated using the optimized parameters between Brokke and Hekni. The solute model was implemented at 5 min time-steps for the river stretch between Rysstad Øy and Straume since oxygen observations were available at these sites. Although the metabolism model implementation in this study is limited to one reach, the model can be extended for multi-reach applications (code available by Pathak, 2022).

Model parameters in the inverse model were estimated using a two-step calibration process (similar to Sincock & Lees, 2002), where flow parameters were first optimized with respect to the observed flow, prior to the optimization of metabolic parameters. Flow parameters can be optimized between the gauging sites on reach-by-reach basis in downstream direction. Flow time-series at Brokke and Hekni were used to first optimize  $F_r$  parameter. Flow at Rysstad Øy and Straume were then modeled using the optimized value of  $F_r$ .

Solute travel times in the River Otra were derived based on velocities as described in Section 3.3 (Table 1). Next, metabolic parameters ( $P_{\text{GPPmax}}$ ,  $k_{\text{PAR}}$ ,  $R_{\text{ER}}$ ) were optimized in the process of fitting oxygen time-series. Model parameters were optimized using a least squares minimization approach with the Nelder-Mead algorithm (Gao & Han, 2012) from the `lmfit` package (v1.0.1) in Python. Lower and upper bounds were provided from prior knowledge to constrain the inverse model parameters and avoid parameter equifinality. Initial values of  $P_{\text{GPP}}$ ,  $k_{\text{PAR}}$ , and  $R_{\text{ER}}$  were provided from the outputs of the two-station accounting method.  $F_{\text{adv}}$  was optimized in the modified two-station model (ADV formulation, accounting method) by minimizing the residual sum of squares of GPP-PAR link function (Equation 16), and was used as a constant in the inverse ADV model. Metabolism parameters were assumed to be constant over a period of 24 hr for a given reach. Summaries of parameters and terms used in different model formulations are provided in Tables S2 and S3 in Supporting Information S1.

We sampled Bayesian posterior distribution of solute model parameters using the Markov Chain Monte Carlo (MCMC) algorithm using the `emcee` package (v3.0.2) in python. This method calculated the log-posterior probability ( $\ln p(\theta_{\text{true}}|D)$ ) of the model parameters ( $\theta$ ) given the data ( $D$ ),

$$\ln p(\theta_{\text{true}}|D) \propto \ln p(\theta_{\text{true}}) - \frac{1}{2} \sum_n \left[ \frac{(g_n(\theta_{\text{true}}) - D_n)^2}{S_n^2} + \ln(2\pi S_n^2) \right] \quad (21)$$

where  $\ln p(\theta_{\text{true}})$  is the log-prior. The second term on the right represents log-likelihood for the  $n$ th observation,  $\ln p(D|\theta_{\text{true}})$ , where  $g_n$  is the generative model,  $D_n$  is the data and  $S_n$  is the measurement uncertainty. Note that we did not use the MCMC algorithm for parameter optimization. Instead, we first optimized the model parameters

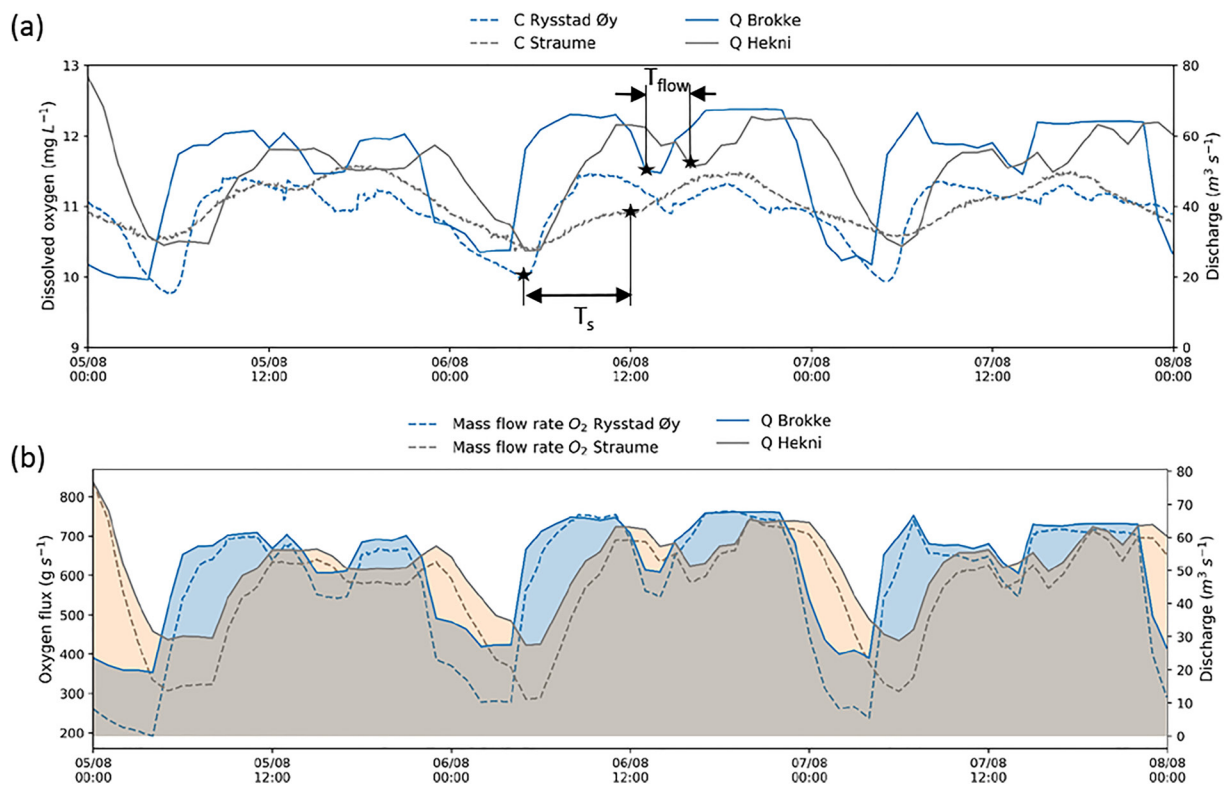


**Figure 3.** Time-series of observed dissolved oxygen concentrations  $C$  and observed flow  $Q$  (interpolated at 5 min interval) (a) and time-series of observed mass flow rate of oxygen and observed flow  $Q$  (interpolated at 5 min interval, line plot with shaded area) at sites within the study stretch (b). Brokke, site 1, Rysstad Øy, site 2, Straume, site 3, Hekni, site 4.  $T_{\text{flow}}$ , travel time of the flood wave;  $T_s$ , solute travel time.

using the Nelder-Mead algorithm and later used the MCMC algorithm to sample from the posterior distribution of these optimized values to obtain parameter uncertainties and covariance.

## 4. Results

Performances of flow routing and metabolism models were evaluated separately. River flows were simulated ahead of the metabolism estimation and outputs from the flow routing model were fed as inputs in the metabolism model. An initial visual inspection of flow and DO curves showed that water traveled faster than DO within the study reach (Figure 3). Such a time lag could result either from the dual water regulation at Brokke and Hekni or from the excessive vegetation in the river reach between Rysstad Øy and Straume. Therefore, to account for this time lag, we included both potential causes in the model formulations that is, pure advection (ADV, Equation 7) and also including transient storage (ADZ, Equation 9) for metabolism estimation. In this section, we present the results of the flow routing and metabolism model applications. Furthermore, we provide posterior probability distribution of optimized model parameters in the inverse metabolism model.

### 4.1. Influence of the Hydropower Plant on DO Dynamics Along the Reach

The O<sub>2</sub> turnover in the second section (sites 2–3) was only 14%, calculated as  $O_{2,\text{turnover}} = 1 - 1/\exp(kL/u)$  (rearranged oxygen footprint equation, Demars et al., 2015), where  $L$  = reach length (4,660 m),  $u$  = average water velocity (8.03 m min<sup>-1</sup>) and  $k$  = gas exchange coefficient (0.00025 min<sup>-1</sup>). The output suggests that 86% of the oxygen variability at Straume (site 3) can be attributed to the variability of oxygen at Rysstad Øy (site 2). It is well known that hydropower operations drive the variability of total dissolved gas at Rysstad Øy (Pulg et al., 2016). Hence, the conventional one-station model (Appling, Hall, Yackulic, & Arroita, 2018; Odum, 1956) or averaged two-station model (Demars, 2019; Demars et al., 2011) would not provide reliable metabolism estimates in the study section (see Text S4 in Supporting Information S1). It also highlights the difficulty of the task of

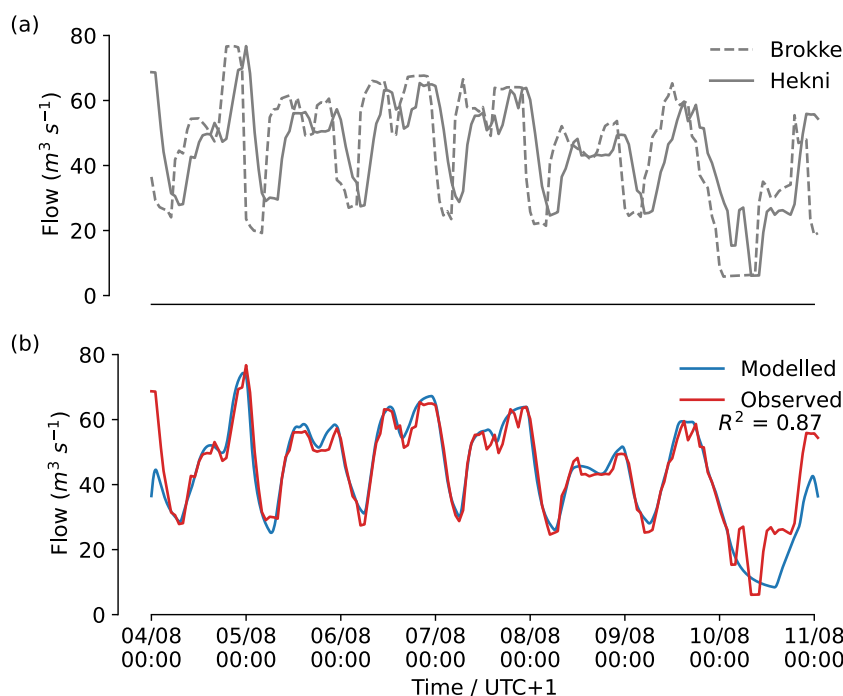


**Figure 4.** Comparison of flow observations at Brokke (site 1) and Hekni (site 4) sites (a) and modeled and observed flows at Hekni site (b) at 5 min time-steps.

disentangling metabolism from background noise, notably the hydropower plant effluent at Brokke representing 87% of median flow that is, most of the  $\text{O}_2$  mass flux.

#### 4.2. Flow Routing Model

The flow routing model was able to capture the timing and magnitude of flow peaks and troughs (Figure 4). The model estimated average 61% retention for flow in the river stretch ( $F_r = 0.61$ ). Minor discrepancies between modeled and observed flows were expected because the flow routing model does not account for the effect of flow regulation at the downstream (Hekni) end that causes rapid rises and falls in water level at Hekni. Nevertheless, the flow routing model satisfactorily reproduced flow variation at Hekni with goodness-of-fit ( $R^2$ ) of 0.87 (Figure 4b).

#### 4.3. Modified Two-Station Model (Accounting Method)

Modified two-station model formulation with only pure advection (ADV) performed better than the formulation with pure advection plus transient storage (ADZ; Figure 5). The two-station ADZ model simulated sudden drops in NEP at Straume around mid-day, suggesting a sudden decrease in GPP around mid-day since ER was assumed to be constant. Variation in PAR did not explain the mid-day drops in GPP (Figure 5c). While an afternoon lull in GPP has often been reported, the estimated mid-day drops in NEP were not driven by biological production, but indicated a systematic error in the metabolism estimates resulting from errors in the simulation of DO mass flux. The mass flux of DO in the river largely followed flow variation. The upstream site (Rysstad Øy) showed concurrent decline in flow and DO in the afternoon owing to changing water demand for power plant operations (Figure 3). The downstream site (Straume) did not show a concurrent decline in DO and flow, but showed shoulders in the DO time-series earlier in the day (around mid-day). These shoulders result from delayed transport of DO from Rysstad Øy to Straume (Figure 3) since oxygen variation at Straume is highly influenced by oxygen variation at Rysstad Øy (explained in Section 4.1). Although the two-station ADZ model accounts for these delayed transport mechanisms through transient storage influence, the modeled NEP did not match our expectation. Better evidence of the ADV model outperforming the ADZ model is presented in Figure 5.

Both models showed a positive relationship between photosynthesis and light, with saturation of photosynthesis under high light intensity (Figure 5). The ADV model ( $R^2 = 0.56$ , Figure 5a) represented a slightly better regression

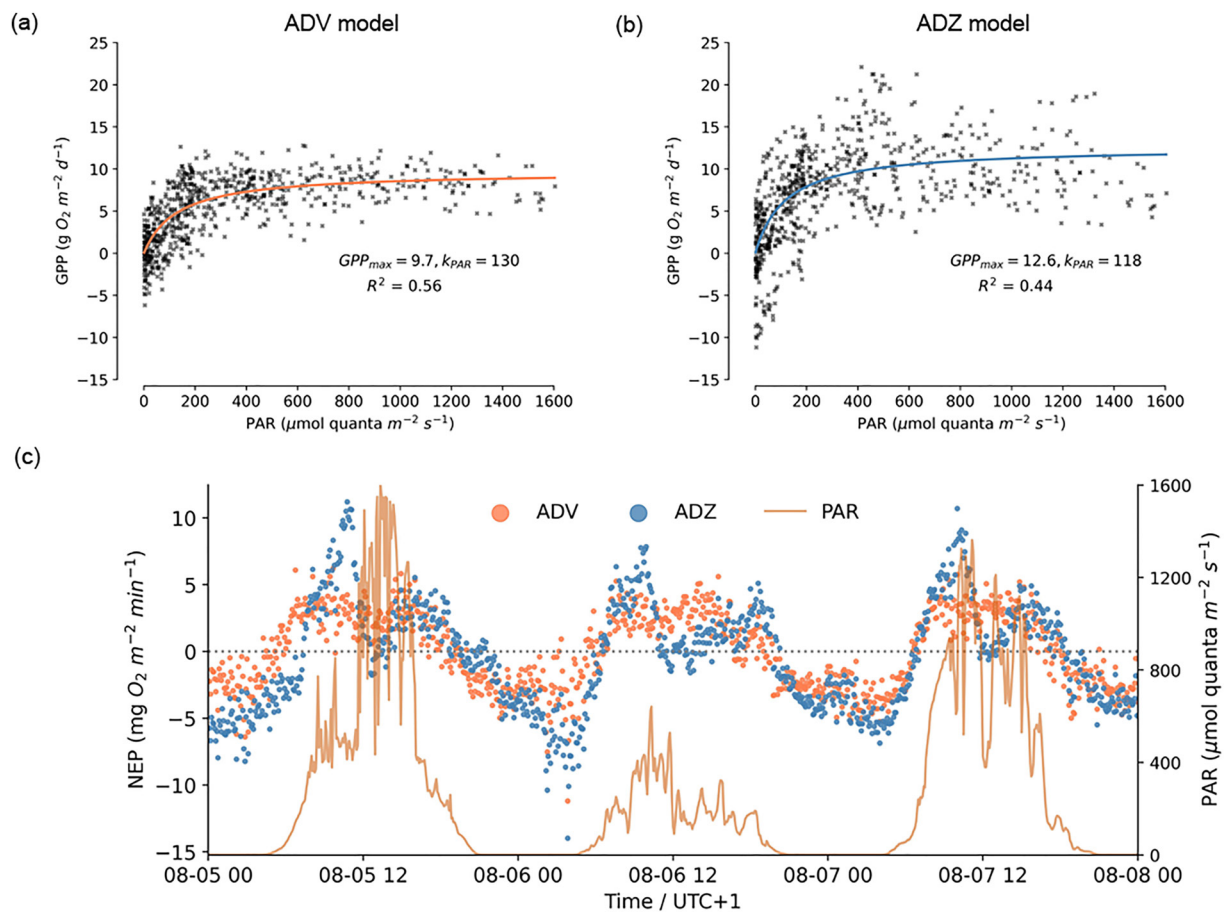


**Figure 5.** Nonlinear regression between gross primary production (GPP) and photosynthetically active radiation (PAR) in the modified two-station (a) ADV and (b) ADZ models at Straume (site 3). (c) shows the variation in net ecosystem production (NEP) and PAR in the modified two-station models at Straume (site 3).

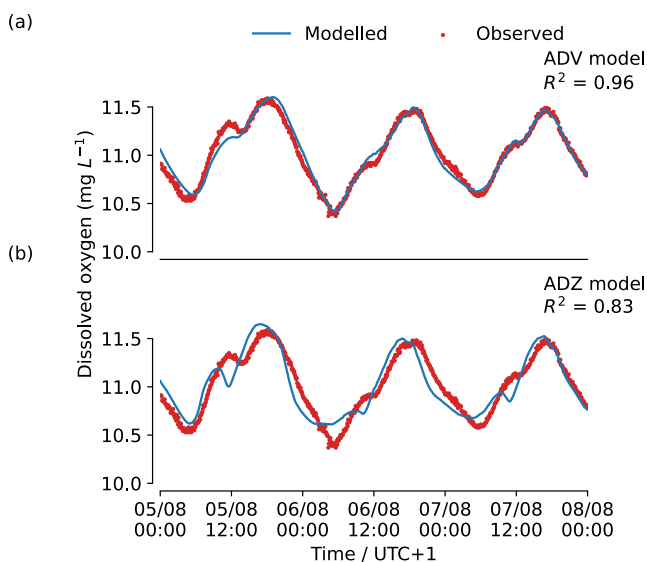


**Figure 6.** Comparison of modeled and observed dissolved oxygen concentrations at 5 min time-steps at Straume (site 3) in the inverse (a) ADV and (b) ADZ formulations.

fit than the ADZ model ( $R^2 = 0.44$ , Figure 5b) for the GPP-PAR link function (Equation 16). The estimates of half-saturation light intensity  $k_{PAR}$  (PAR at which half the maximum GPP is attained) in both models (Figure 5) were in line with what is commonly observed in freshwater systems ( $k_{PAR} = 100\text{--}500 \mu\text{mol-phons } m^{-2} s^{-1}$ , Demars et al., 2011). The estimates of  $P_{GPPmax}$  and  $k_{PAR}$  fitted in the GPP-PAR link function (Figure 5) served as priors in the inverse model when simulating GPP as a function of PAR.

#### 4.4. Inverse Metabolism Model

Both ADV and ADZ formulations captured the overall DO variation at Straume (Figure 6), but the ADV model performed significantly better than the ADZ model to capture the overall trend and magnitude of oxygen variation. The ADZ model showed a small time lag between the observed and modeled DO concentrations, which indicates inaccuracies in the simulation of DO mass flux with flow. Note that the flow-velocity relationships derived for TDG in the study reach do not cover the entire range of observed flows during the modeling period (e.g., equations derived for velocities at  $Q > 50 m^3 s^{-1}$  for reach 2, Figure S2 in Supporting Information S1).

Estimated values of metabolism parameters in the ADV model are generally lower than the estimates of the ADZ model (Table S4 in Supporting Information S1). The ADV model ( $R^2 = 0.96$ ) derived a better overall

**Table 2**

*Median Values of Posterior Probability Distribution of the Inverse ADV Model Parameters With  $1 - \sigma$  Uncertainty Derived From the Markov Chain Monte Carlo Runs and Optimized Parameter Values by the Nelder-Mead Least Squares Minimization Algorithm (in Brackets)*

Parameter	Day 1	Day 2	Day 3
$P_{\text{GPPmax}}$	$8.64 \pm 0.16$ (8.64)	$12.38 \pm 0.12$ (12.96)	$11.52 \pm 0.24$ (11.52)
$k_{\text{PAR}}$	$144 \pm 5$ (144)	$144 \pm 1$ (144)	$461 \pm 32$ (461)
$R_{\text{ER}}$	$3.46 \pm 0.09$ (3.46)	$4.61 \pm 0.05$ (4.32)	$4.03 \pm 0.04$ (4.03)

*Note.* Units are  $\text{g O}_2 \text{ m}^{-2} \text{ d}^{-1}$  for  $P_{\text{GPPmax}}$  and  $R_{\text{ER}}$ , and  $\mu\text{mol-photon m}^{-2} \text{ s}^{-1}$  for  $k_{\text{PAR}}$ .

goodness-of-fit than the ADZ model ( $R^2 = 0.83$ ). Therefore, we selected the ADV model to sample Bayesian posterior distribution of metabolism parameters using the MCMC algorithm.  $P_{\text{GPPmax}}$  and  $R_{\text{ER}}$  parameters showed a strong positive correlation during the first 2 days of the modeling period ( $>0.86$ ). Other significant correlations were observed for half-saturation light intensity with maximum GPP ( $k_{\text{PAR}}-P_{\text{GPPmax}}$ , 0.95) and with respiration rate ( $k_{\text{PAR}}-R_{\text{ER}}$ ,  $-0.63$ ) on the third day. Despite these high correlations, we find that the median values (and maximum likelihood estimates) of all metabolism parameters lie in a close range of the values optimized by the Nelder-Mead minimization algorithm (within  $1 - \sigma$  uncertainty; Table 2, Figure 7). The performance of the MCMC algorithm was judged using the estimate of average acceptance fraction, which was found to be within an acceptable range (0.2–0.5, Foreman-Mackey et al., 2013) in all cases. Figure 8 shows the variation in NEP and the relationship between GPP-PAR as estimated in the inverse ADV model.

## 5. Discussion

The MUFT model application here demonstrates how the impact of hydropeaking (i.e., sub-daily flow fluctuations) and transient storage can be included in the estimation of metabolism. Commonly used one-station models are not suitable for river reaches with large discontinuities (e.g., hydropower dams, waste water treatment plants; Appling, Hall, Yackulic, & Arroita, 2018; Demars et al., 2015). In such cases, two-station models are advantageous, but are not completely immune to flow fluctuations during the period of analysis (Hall et al., 2016) and work only at a river reach scale (Demars et al., 2015). Additionally, these models do not account for the influence of transient storage on DO transport in river reaches. The MUFT model addresses these limitations by coupling an unsteady flow routing model with the two-station metabolism method, modified to account for transient storage zones. The model simulates river reaches as cells connected in series with advection time delay and thus, it is possible to estimate metabolism at a larger spatial scale including at sites where continuous DO observations are not available, but observations of other environmental variables are available (e.g., Pathak et al., 2022; Segatto et al., 2020). The model structure allows translation of upstream changes in river flow and quality dynamics (e.g., hydropeaking, pollution loading) to downstream sites of interest. Therefore, future model users may test its application for ecological assessments in response to river regulation/restoration actions under changing environmental conditions. A comparison of MUFT model performance with the commonly used one-station and two-station models is demonstrated in Text S4, Figure S6, and Table S5 in Supporting Information S1.

MUFT model application requires continuous time-series of DO, discharge, water temperature and atmospheric pressure at a minimum of two sites in the river reach for model input and calibration. PAR is also crucial and ideally should be measured at the river site. However, when PAR measurements are not feasible, it can be modeled using remote sensing information (Hall et al., 2015; Holtgrieve et al., 2010; Waylett et al., 2013). Accurate estimation of mean velocity and solute residence time is important, especially in river reaches with significant transient storage (Lees et al., 2000). Ideally, a conservative tracer such as salt slug (Hall & Hotchkiss, 2017) should be used to derive residence time and velocity estimates, but other approaches (e.g., use of TDG as shown here) may be employed if estimates can be validated with observations. Furthermore, tracer experiments for varying discharge may help derive empirical relationships between discharge and velocity, which is useful for upscaling metabolism estimates (Raymond et al., 2012).

The model can be applied using an accounting method (book-keeping) and/or inverse modeling approach. The model also allows flexibility in selecting an appropriate model structure to suit hydrological and solute transport characteristics in the river, as demonstrated here with the application of ADV and ADZ models in the River

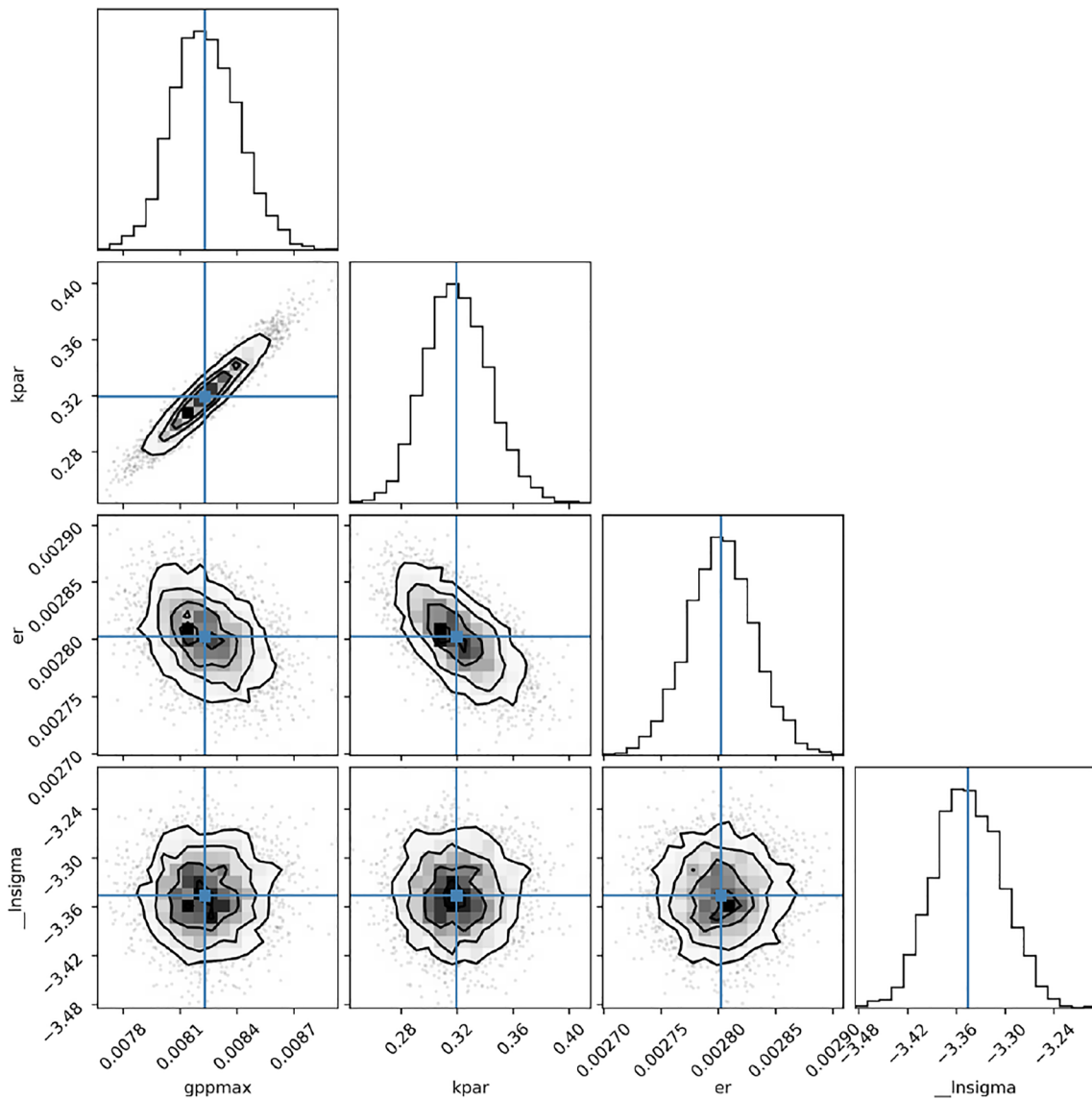


**Figure 7.** Posterior distribution of inverse ADV model parameters gppmax ( $P_{GPPmax}$ , maximum gross primary production), kpar ( $k_{PAR}$ , half-saturation light intensity), and er ( $R_{ER}$ , ecosystem respiration) using Markov Chain Monte Carlo algorithm on day 3 at Straume (site 3). Blue lines show the median values of posterior probability distribution of model parameters. \_Insigma parameter is used to estimate the true uncertainty in the data.

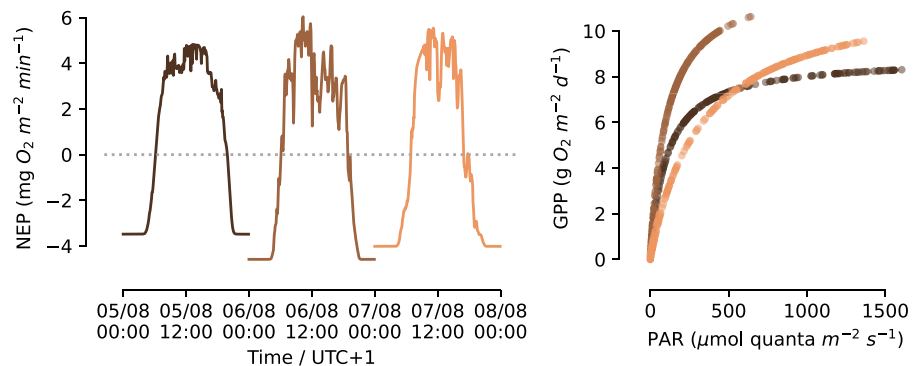


**Figure 8.** Estimated net ecosystem production (NEP) (a) and modeled GPP-PAR relationship (b) at Straume (site 3) in the inverse ADV model. GPP, gross primary production and PAR, photosynthetically active radiation.

Otra. The better performance of the ADV model compared to the ADZ model in our case study suggests that despite the initial hypothesis, vegetation may not produce significant transient storage (ADZ) in the river and that introduction of pure transportation delay (ADV) in the model may be sufficient to characterize DO dynamics at Straume during the modeling period. Due to limited data availability, it is difficult to confidently pinpoint the dominant transport mechanism in the river. The dominant transport mechanism in rivers may differ with varying discharge, channel morphology, and bed composition. For example, ADZ model may be required in larger gravel bed rivers with extensive hyporheos or rivers with vegetated side pools. Since, this study aims to present a general model application for metabolism estimation, we do not delve in to the specifics of the process-dynamics in the River Otra. Nevertheless, a comparative modeling approach such as MUFT may help identify where the ADV or ADZ model is required to explain river oxygen dynamics. In the following sub-sections, we discuss the differences in the MUFT inverse and accounting modeling approaches along with their limitations and the possibilities of future model improvements.

### 5.1. Comparison of the Inverse Model With the Modified Two-Station Model

Discrepancies in the outputs of the inverse and modified two-station models mainly arise from the differences in the model structures. For example, the numerical solution of the ODE equation in the modified two-station model uses a simple Euler finite difference scheme as opposed to a more robust lsoda solver from the FORTRAN library odepack (Hindmarsh, 1983) in the inverse model. Moreover, both models characterize GPP in different ways. The accounting approach, although advantageous for not assuming the type of relationship between GPP and PAR, may fail to segregate the influence of flow on DO mass flux from the influence of biological production on DO transformations, when DO mass flux and/or solute-lag coefficient are not characterized accurately. On the other hand, the inverse model is able to segregate these influences up to a certain extent because GPP is modeled as a function of PAR.

Another difference between the two approaches is the parameter calibration process. The two-station method involves an accounting approach where NEP is directly estimated from oxygen observations without any parameter calibration procedure. Daily average ER is then estimated during dark hours, and GPP is calculated as a difference between NEP and daily average ER. The inverse model, on the other hand, optimizes model parameters in the process of fitting modeled DO to observed DO time-series using a least squares minimization algorithm; hence, providing more confidence in the model estimates. Admittedly, the inverse approach includes more number of model parameters, corresponding to a larger number of degrees of freedom and consequently, the risk of parameter equifinality (Spear & Hornberger, 1980). However, as demonstrated in this study, equifinality may be reduced by constraining the parameter space with prior knowledge of the river system and by minimizing the number of unknown parameters by using field measurements to the extent feasible (e.g., Du et al., 2014). Often, random sampling methods such as MCMC algorithms are useful to estimate uncertainty in the optimized model parameters (e.g., Segatto et al., 2021) as represented in this study. Furthermore, sensitivity analysis may also be used to identify the most influential parameters for the simulations (e.g., Vandenberghe et al., 2001).

Although the modified two-station approach is simpler and quicker compared to the inverse model, its application is limited to a much smaller spatial scale, that is, river-reach scale. Additionally, the two-station accounting approach relies on continuous DO measurements at both sites in the river reach of interest, which is often not possible due to adverse field conditions, drifting of sensors, etc (Wagner et al., 2006). On the contrary, the inverse model is an apt alternative to estimate long-term trends in metabolism at a river-network scale even when there are gaps present in continuous DO measurements at calibration sites. Despite the differences laid out here, we showed that the outcomes from the two-station accounting approach are useful to constrain the metabolism parameters in the inverse model. Therefore, both approaches are complementary rather than competitive.

### 5.2. Modeling Limitations and Future Efforts

The parsimonious model MUFT relies on certain assumptions. For example, the flow routing model approximates constant flow parameters for the entire reach between Brokke and Hekni because it employs reach-by-reach calibration method between gauging stations. In this study, a constant retention parameter was assumed for the entire river section between Brokke and Hekni. This assumption is not realistic since river hydraulics vary within the stretch (discussed in Section 3.3). Although we accounted for heterogeneity using reach-wise flow-velocity

relationships in the flow routing model, such data may not be easily available in other rivers. It is important to estimate flow parameters precisely because small errors in flow parameters may result in large errors in metabolism estimates when flow dominates the mass flux of oxygen in the river. Multiple nonlinear storage tanks ( $n_c > 1$ ) may be more appropriate when the river section is heterogeneous, but increasing  $n_c$  value did not significantly improve model performance in this case. Parameter sensitivity analysis (e.g., Sincock et al., 2003) may also be employed prior to MCMC simulations to identify an appropriate model structure and reduce bias in the flow parameters. However, a more detailed investigation of parameter bias is out of the scope of this study.

It is difficult to derive a physical understanding of travel time mechanisms because of the lumped parameter structure of the MUFT model. Characterization of oxygen travel time from flow-based parameters integrates flow and metabolism models and therefore, overcomes this issue to a certain extent. However, it is still difficult to relate travel time parameters to river hydraulic properties and interpret the physical significance of model coefficients because of the crude description of dead zone (ADZ, Wallis et al., 1989) and advective transport (ADV, Beck, 1976) in the model. For example, we found ADZ residence time to be poorly related to metabolism. A lack of a strong relationship may partly be attributed to the assumption that TDG velocity  $\approx$  solute velocity in the river. This assumption may introduce some bias in NEP estimates. Conservative tracer experiments may help characterize solute travel time parameters (e.g.,  $T_{\text{sadz}}$ ,  $T_{\text{adz}}$ ,  $\beta$ ) more accurately and consequently, help reduce the bias in metabolism estimates. A poor relationship may also occur from model's inability to account for the diversity of transient storage components that contribute to different metabolic processes (e.g., autotrophic and heterotrophic production; Haggerty et al., 2009). One way to account for diverse transient storage zones is through resazurin tracer experiments, to segregate metabolically active transient storage from a less-active transient storage (Argerich et al., 2011; Haggerty et al., 2009). However, the possibility of a weak or non-existent relationship between transient storage and ecosystem functioning cannot be neglected (Bernhardt et al., 2002; Webster et al., 2003). Nonetheless, in spite of limited available data and a simplified structure, both formulations of the model are able to provide fairly accurate predictions of oxygen transport and dispersion in this as well as previous studies (Lees et al., 2000; Santos Santos & Camacho, 2022). The MUFT model thus offers an alternative with a trade-off between accuracy and complexity.

Another simplification in the MUFT model is in the way in-stream processes are modeled. The ADZ formulation, in particular, assumes that metabolic activity occurs in the transient storage zone, and not during oxygen advection. Lees et al. (1998) proposed a mass decay term for non-conservative solutes (e.g., ammonium). However, it is difficult to characterize mass decay of oxygen during advection through a single term, when coupled with stream metabolism approach. On the other hand, the ADV formulation does not have this issue since it assumes that advection process is dominant in the river reach. The model also includes a simple formulation of metabolism fluxes, but a more complex formulation may be included if necessary. We find that a Michaelis-Menten type equation adequately simulates GPP in the River Otra, but the model can be easily modified to include other formulations such as linear (Payn et al., 2017) or hyperbolic tangent function (Holtgrieve et al., 2010; Jassby & Platt, 1976). We assume constant ER over a day to keep the model structure simple, but ER may be varied as a function of water temperature (Holtgrieve et al., 2010; Song et al., 2018) if deemed necessary in the river system. Estimate of gas-exchange coefficient  $k$  is crucial since a small bias in  $k$  may lead to a large bias in metabolism estimates (Hall & Ulseth, 2020).  $k$  may be modeled as a function of river hydraulic properties (Raymond et al., 2012) or may be estimated during model calibration with prior information from empirical relationships or direct measurements (Holtgrieve et al., 2010). Here,  $k$  is estimated from floating chamber studies, performed under a limited range of flows. Use of a constant  $k$  value during the modeling period was adequate in this case because the study reach represented slow-flowing water with considerably low gas-exchange compared to metabolism, thus limiting biases in metabolism from biases in  $k$ .

A full dynamic flood wave routing, based on Saint-Venant's equations and commonly used in one-dimensional hydrological models, is suitable in unsteady flow conditions. The MUFT model uses a simpler flow routing model (Sincock & Lees, 2002) than a dynamic wave routing model (see Payn et al., 2017). The long reaches and time-steps ( $T_s$ ,  $t - \alpha$ ,  $t - \tau_s$ ) in the MUFT model create a physical anomaly that is, the advection delays ( $\alpha$  for ADV,  $\tau_s$  for ADZ) increase when discharge drops and thus the time-step terms  $t - \alpha$  and  $t - \tau_s$  at time  $t$  "look" further back in time as time progresses (see Figure S7 in Supporting Information S1). The discretization procedure of Payn et al. (2017) is likely a more accurate procedure to estimate metabolism than MUFT, but at the cost of extra complexity. Similarly, transient storage models generally use one-dimensional, advection-dispersion equations (Bencala & Walters, 1983; Runkel, 1998) to simulate solute movement, albeit assuming steady flows

or estimating transient storage under different flow volumes (e.g., Manson et al., 2010). The MUFT model, on the other hand, takes a simpler approach by characterizing river reaches as nonlinear storage zones in series (zero-dimensional), and simulates water and solute movement using ordinary differential equations. The choice of a simpler structure in the MUFT model is beneficial because different modules (e.g., flow routing, transient storage zone, and metabolism) of the model are compatible, and because the model offers benefits of reduced complexity (zero-dimensional) with less number of model parameters over one-dimensional hydrological and solute models. Reduced complexity in models is advantageous since it minimizes data requirements, model sensitivity, and issues of parameter equifinality (Lindenschmidt, 2006).

## 6. Summary and Conclusion

This study presents a coupled modeling approach (MUFT) to estimate whole-stream metabolism in rivers with unsteady flow conditions and transient storage zones. The MUFT model integrates flow and oxygen modeling based on travel-time relationships proposed by Sincock and Lees (2002), which were originally built on QUASAR (Whitehead et al., 1997) and ADZ (Lees et al., 2000; Wallis et al., 1989) model equations. We propose an additional model formulation for dominant advective transport (ADV) based on the model developed by Beck and Young (1975). The MUFT approach can be applied through inverse modeling or accounting method (two-station method) according to user's preference and data availability. We demonstrated the application of the MUFT model in the River Otra in southern Norway. We found that the accounting method is simpler, but shows high bias in metabolism estimates when oxygen mass flux is not precisely modeled. The inverse modeling approach is more robust as it employs least squares minimization algorithm to optimize model parameters. Moreover, the inverse model supports investigation of parameter uncertainties and correlations through Bayesian sampling of posterior distributions.

The MUFT approach presents opportunities to estimate whole-stream metabolism in hydropeaking river environments as well as in rivers influenced by transient storage zones. With increasing feasibility of high-resolution, long-term oxygen monitoring in rivers (Appling, Hall, Yackulic, & Arroita, 2018; Appling et al., 2018; Bernhardt et al., 2022), it is possible to extend the model for network-scale metabolism prediction. Using the knowledge of river hydraulics, the inverse model may also be able to predict metabolism rates at sites within the river network where continuous monitoring is not carried out (e.g., Pathak et al., 2022). In future, the model can be implemented for metabolism prediction under changes such as warming, extreme weather events, and river management practices—a research area that calls for more attention (Bernhardt et al., 2018).

### Acknowledgments

The authors thank Otra Kraft for providing flow data and boats; Ulrich Pulg and Sebastian Stranzl for providing TDG data and lime addition data; Peter Dörsch for CO<sub>2</sub> GC analyses; Odd Arne Skogan for setting up the Campbell logging station; Knut Olav Oppstad for providing sonar bathymetric data; Kirstine Thiemer, Susanne Schneider, Emmanuel Bergan, Astrid Torske, Eirin Aasland for help collecting bathymetric and plant data, as well as CO<sub>2</sub> flux with the floating chambers. BOLD gratefully acknowledges the Research Council of Norway (297202/E10), the German Federal Ministry of Education and Research (033WU005), the French Agence National de Recherche (N° ANR-18-IC4W-0004-06), and the South African Water Research Commission (K5/2951) for funding of MadMacs (Mass development of aquatic macrophytes - causes and consequences of macrophyte removal for ecosystem structure, function, and services) in the frame of the collaborative international consortium of the 2017 call of the Water Challenges for a Changing World Joint Programme Initiative (Water JPI). Additional funding was provided by Krypsiv på Sørlandet and the Norwegian institute for water research (NIVA). D.P. acknowledges the funding from the European Union's Horizon 2020 research and innovation program under the Marie Skłodowska-Curie grant agreement no. 765553.

### Data Availability Statement

v0.1.0 of the MUFT model developed for metabolism estimation and data used in the model development and application are preserved at <https://doi.org/10.5281/zenodo.7197544>, available via Creative Commons Attribution 4.0 International license and developed at <https://github.com/d-pathak/MUFT-model/tree/v0.1.0> (Pathak, 2022).

### References

- Appling, A. P., Hall, R. O., Jr., Yackulic, C. B., & Arroita, M. (2018). Overcoming equifinality: Leveraging long time series for stream metabolism estimation. *Journal of Geophysical Research: Biogeosciences*, 123(2), 624–645. <https://doi.org/10.1002/2017jg004140>
- Appling, A. P., Read, J. S., Winslow, L. A., Arroita, M., Bernhardt, E. S., Griffiths, N. A., et al. (2018). The metabolic regimes of 356 rivers in the United States. *Scientific Data*, 5(1), 1–14. <https://doi.org/10.1038/sdata.2018.292>
- Argerich, A., Haggerty, R., Martí, E., Sabater, F., & Zarnetske, J. (2011). Quantification of metabolically active transient storage (MATS) in two reaches with contrasting transient storage and ecosystem respiration. *Journal of Geophysical Research*, 116(G3), G03034. <https://doi.org/10.1029/2010jg001379>
- Aristi, I., Arroita, M., Larrañaga, A., Ponsatí, L., Sabater, S., von Schiller, D., et al. (2014). Flow regulation by dams affects ecosystem metabolism in Mediterranean rivers. *Freshwater Biology*, 59(9), 1816–1829. <https://doi.org/10.1111/fwb.12385>
- Ashraf, F. B., Haghighi, A. T., Riml, J., Alfredsen, K., Koskela, J. J., Kløve, B., & Marttila, H. (2018). Changes in short-term river flow regulation and hydropeaking in Nordic rivers. *Scientific Reports*, 8(1), 1–12. <https://doi.org/10.1038/s41598-018-35406-3>
- Bastviken, D., Sundgren, I., Natchimuthu, S., Reyier, H., & Gålfalk, M. (2015). Cost-efficient approaches to measure carbon dioxide (CO<sub>2</sub>) fluxes and concentrations in terrestrial and aquatic environments using mini loggers. *Biogeosciences*, 12(12), 3849–3859. <https://doi.org/10.5194/bg-12-3849-2015>
- Battin, T. J., Lauerwald, R., Bernhardt, E. S., Bertuzzo, E., Gener, L. G., Hall, R. O., Jr., et al. (2023). River ecosystem metabolism and carbon biogeochemistry in a changing world. *Nature*, 613(7944), 449–459. <https://doi.org/10.1038/s41586-022-05500-8>
- Beck, M. (1976). Dynamic modeling and control applications in water quality maintenance. *Water Research*, 10(7), 575–595. [https://doi.org/10.1016/0043-1354\(76\)90139-1](https://doi.org/10.1016/0043-1354(76)90139-1)

- Beck, M., & Young, P. C. (1975). A dynamic model for DO—BOD relationships in a non-tidal stream. *Water Research*, 9(9), 769–776. [https://doi.org/10.1016/0043-1354\(75\)90028-7](https://doi.org/10.1016/0043-1354(75)90028-7)
- Beer, T., & Young, P. C. (1983). Longitudinal dispersion in natural streams. *Journal of Environmental Engineering*, 109(5), 1049–1067. [https://doi.org/10.1061/\(asce\)0733-9372\(1983\)109:5\(1049\)](https://doi.org/10.1061/(asce)0733-9372(1983)109:5(1049))
- Bencala, K. E., & Walters, R. (1983). Simulation of solute transport in a mountain pool-and-riffle stream—A transient storage model. *Water Resources Research*, 19(3), 718–724. <https://doi.org/10.1029/wr019i003p00718>
- Bernhardt, E. S., Hall, R. O., Jr., & Likens, G. E. (2002). Whole-system estimates of nitrification and nitrate uptake in streams of the Hubbard Brook Experimental Forest. *Ecosystems*, 5(5), 419–430. <https://doi.org/10.1007/s10021-002-0179-4>
- Bernhardt, E. S., Heffernan, J. B., Grimm, N. B., Stanley, E. H., Harvey, J., Arroita, M., et al. (2018). The metabolic regimes of flowing waters. *Limnology & Oceanography*, 63(S1), S99–S118. <https://doi.org/10.1002/lno.10726>
- Bernhardt, E. S., Savoy, P., Vlah, M. J., Appling, A. P., Koenig, L. E., Hall, R. O., et al. (2022). Light and flow regimes regulate the metabolism of rivers. *Proceedings of the National Academy of Sciences*, 119(8). <https://doi.org/10.1073/pnas.2121976119>
- Borges, A. V., Darchambeau, F., Lambert, T., Morana, C., Allen, G. H., Tambwe, E., et al. (2019). Variations in dissolved greenhouse gases (CO<sub>2</sub>, CH<sub>4</sub>, N<sub>2</sub>O) in the Congo river network overwhelmingly driven by fluvial-wetland connectivity. *Biogeosciences*, 16(19), 3801–3834. <https://doi.org/10.5194/bg-16-3801-2019>
- Bottacin-Busolin, A., Singer, G., Zaramella, M., Battin, T. J., & Marion, A. (2009). Effects of streambed morphology and biofilm growth on the transient storage of solutes. *Environmental Science & Technology*, 43(19), 7337–7342. <https://doi.org/10.1021/es900852w>
- Chapra, S. C. (2008). *Surface water-quality modeling*. Waveland Press.
- Chapra, S. C., & Runkel, R. L. (1999). Modeling impact of storage zones on stream dissolved oxygen. *Journal of Environmental Engineering*, 125(5), 415–419. [https://doi.org/10.1061/\(asce\)0733-9372\(1999\)125:5\(415\)](https://doi.org/10.1061/(asce)0733-9372(1999)125:5(415))
- Chowanski, K., Kunza, L., Hoffman, G., Genzoli, L., & Stickney, E. (2020). River management alters ecosystem metabolism in a large oligotrophic river. *Freshwater Science*, 39(3), 534–548. <https://doi.org/10.1086/710082>
- Cimorelli, L., Cozzolino, L., D'Aniello, A., Morlando, F., Pianese, D., & Singh, V. (2016). A new semi-Lagrangian routing procedure for constituent transport in steady and unsteady flow velocity fields. *Journal of Hydrology*, 538, 216–230. <https://doi.org/10.1016/j.jhydrol.2016.04.022>
- Cox, B. (2003a). A review of currently available in-stream water-quality models and their applicability for simulating dissolved oxygen in lowland rivers. *Science of the Total Environment*, 314, 335–377. [https://doi.org/10.1016/s0048-9697\(03\)00063-9](https://doi.org/10.1016/s0048-9697(03)00063-9)
- Cox, B. (2003b). A review of dissolved oxygen modeling techniques for lowland rivers. *Science of the Total Environment*, 314, 303–334. [https://doi.org/10.1016/s0048-9697\(03\)00062-7](https://doi.org/10.1016/s0048-9697(03)00062-7)
- Davidson, J. (1957). The determination of diffusion coefficient for sparingly soluble gases in liquids. *Transactions of the American Institute of Chemical Engineers*, 35, 51–60.
- Demars, B. O. L. (2019). Hydrological pulses and burning of dissolved organic carbon by stream respiration. *Limnology & Oceanography*, 64(1), 406–421. <https://doi.org/10.1002/lno.11048>
- Demars, B. O. L., Dörsch, P., Thiemer, K., Clayner, K., Schneider, S. C., Stranzl, S. F., et al. (2021). *Hydropower: Gas supersaturation and the role of aquatic plant photosynthesis for fish health (Tech. Rep. No. 7633-2021)*. Norwegian Institute for Water Research
- Demars, B. O. L., Russell Manson, J., Olafsson, J. S., Gislason, G. M., Gudmundsdóttir, R., Woodward, G., et al. (2011). Temperature and the metabolic balance of streams. *Freshwater Biology*, 56(6), 1106–1121. <https://doi.org/10.1111/j.1365-2427.2010.02554.x>
- Demars, B. O. L., Thompson, J., & Manson, J. R. (2015). Stream metabolism and the open diel oxygen method: Principles, practice, and perspectives. *Limnology and Oceanography: Methods*, 13(7), 356–374. <https://doi.org/10.1002/lom3.10030>
- Du, E., Link, T. E., Gravelle, J. A., & Hubbard, J. A. (2014). Validation and sensitivity test of the distributed hydrology soil-vegetation model (DHSVM) in a forested mountain watershed. *Hydrological Processes*, 28(26), 6196–6210. <https://doi.org/10.1002/hyp.10110>
- Ensign, S. H., & Doyle, M. W. (2005). In-channel transient storage and associated nutrient retention: Evidence from experimental manipulations. *Limnology & Oceanography*, 50(6), 1740–1751. <https://doi.org/10.4319/lno.2005.50.6.1740>
- Fellows, C. S., Valett, M. H., & Dahm, C. N. (2001). Whole-stream metabolism in two montane streams: Contribution of the hyporheic zone. *Limnology & Oceanography*, 46(3), 523–531. <https://doi.org/10.4319/lno.2001.46.3.0523>
- Ferreira, V., Eloşegi, A., D Tiegş, S., von Schiller, D., & Young, R. (2020). Organic matter decomposition and ecosystem metabolism as tools to assess the functional integrity of streams and rivers—A systematic review. *Water*, 12(12), 3523. <https://doi.org/10.3390/w12123523>
- Foreman-Mackey, D., Hogg, D. W., Lang, D., & Goodman, J. (2013). emcee: The MCMC hammer. *Publications of the Astronomical Society of the Pacific*, 125(925), 306–312. <https://doi.org/10.1086/670067>
- Gao, F., & Han, L. (2012). Implementing the Nelder-Mead simplex algorithm with adaptive parameters. *Computational Optimization and Applications*, 51(1), 259–277. <https://doi.org/10.1007/s10589-010-9329-3>
- Haggerty, R., Martí, E., Argerich, A., Von Schiller, D., & Grimm, N. B. (2009). Resazurin as a “smart” tracer for quantifying metabolically active transient storage in stream ecosystems. *Journal of Geophysical Research: Biogeosciences*, 114(G3), G03014. <https://doi.org/10.1029/2008jg000942>
- Hall, R. O., Jr., & Hotchkiss, E. R. (2017). Stream metabolism. In *Methods in stream ecology* (pp. 219–233). Elsevier.
- Hall, R. O., Jr., Tank, J. L., Baker, M. A., Rosi-Marshall, E. J., & Hotchkiss, E. R. (2016). Metabolism, gas exchange, and carbon spiraling in rivers. *Ecosystems*, 19(1), 73–86. <https://doi.org/10.1007/s10021-015-9918-1>
- Hall, R. O., Jr., & Ulseth, A. J. (2020). Gas exchange in streams and rivers. *Wiley Interdisciplinary Reviews: Water*, 7(1), e1391. <https://doi.org/10.1002/wat2.1391>
- Hall, R. O., Jr., Yackulic, C. B., Kennedy, T. A., Yard, M. D., Rosi-Marshall, E. J., Voichick, N., & Behn, K. E. (2015). Turbidity, light, temperature, and hydropeaking control primary productivity in the Colorado River, Grand Canyon. *Limnology & Oceanography*, 60(2), 512–526. <https://doi.org/10.1002/lno.10031>
- Hindmarsh, A. C. (1983). ODEPACK, a systematized collection of ode solvers. *Scientific Computing*, 55–64.
- Holtgrieve, G. W., Schindler, D. E., Branch, T. A., & A'mar, Z. T. (2010). Simultaneous quantification of aquatic ecosystem metabolism and reaeration using a Bayesian statistical model of oxygen dynamics. *Limnology & Oceanography*, 55(3), 1047–1063. <https://doi.org/10.4319/lno.2010.55.3.1047>
- Holtgrieve, G. W., Schindler, D. E., & Jankowski, K. (2016). Comment on Demars et al. 2015, “stream metabolism and the open diel oxygen method: Principles, practice, and perspectives”. *Limnology and Oceanography: Methods*, 14(2), 110–113. <https://doi.org/10.1002/lom3.10075>
- Hotchkiss, E., Hall, R., Jr., Sponseller, R., Butman, D., Klaminder, J., Laudon, H., et al. (2015). Sources of and processes controlling CO<sub>2</sub> emissions change with the size of streams and rivers. *Nature Geoscience*, 8(9), 696–699. <https://doi.org/10.1038/ngeo2507>
- Jassby, A. D., & Platt, T. (1976). Mathematical formulation of the relationship between photosynthesis and light for phytoplankton. *Limnology & Oceanography*, 21(4), 540–547. <https://doi.org/10.4319/lno.1976.21.4.0540>

- Koschorreck, M., Prairie, Y. T., Kim, J., & Marcé, R. (2021). CO<sub>2</sub> is not like CH<sub>4</sub>—limits of and corrections to the headspace method to analyze PCO<sub>2</sub> in water. *Biogeosciences*, 18(5), 1619–1627. <https://doi.org/10.5194/bg-18-1619-2021>
- Kurz, M. J., Drummond, J. D., Martí, E., Zarnetske, J. P., Lee-Cullin, J., Klaar, M. J., et al. (2017). Impacts of water level on metabolism and transient storage in vegetated lowland rivers: Insights from a mesocosm study. *Journal of Geophysical Research: Biogeosciences*, 122(3), 628–644. <https://doi.org/10.1002/2016jg003695>
- Lees, M. J., & Camacho, L. (2000). Modeling solute transport in rivers under unsteady flow conditions—An integrated velocity conceptualization. British Hydrological Society. In *Seventh National Hydrology Symposium* (pp. 4–6). Newcastle.
- Lees, M. J., Camacho, L. A., & Chapra, S. (2000). On the relationship of transient storage and aggregated dead zone models of longitudinal solute transport in streams. *Water Resources Research*, 36(1), 213–224. <https://doi.org/10.1029/1999wr900265>
- Lees, M. J., Camacho, L., & Whitehead, P. (1998). Extension of the quasar river water quality model to incorporate dead-zone mixing. *Hydrology and Earth System Sciences*, 2(2/3), 353–365. <https://doi.org/10.5194/hess-2-353-1998>
- Lindenschmidt, K.-E. (2006). The effect of complexity on parameter sensitivity and model uncertainty in river water quality modeling. *Ecological Modeling*, 190(1–2), 72–86. <https://doi.org/10.1016/j.ecolmodel.2005.04.016>
- Manson, J., Demars, B., Wallis, S., & Mynik, V. (2010). A combined computational and experimental approach to quantifying habitat complexity in Scottish upland streams. *Proceedings of Hydropredict*.
- Manson, J., Wallis, S. G., & Hope, D. (2001). A conservative semi-Lagrangian transport model for rivers with transient storage zones. *Water Resources Research*, 37(12), 3321–3329. <https://doi.org/10.1029/2001wr002230>
- Martinsen, K. T., Kragh, T., & Sand-Jensen, K. (2018). A simple and cost-efficient automated floating chamber for continuous measurements of carbon dioxide gas flux on lakes. *Biogeosciences*, 15(18), 5565–5573. <https://doi.org/10.5194/bg-15-5565-2018>
- Moe, T. F., & Demars, B. O. L. (2017). *Årsrapport krysivovervåking 2017 (Tech. Rep. No. 7202-2017)*. Norsk Institutt for Vannforskning.
- Mulholland, P., Fellows, C., Tank, J., Grimm, N., Webster, J., Hamilton, S., et al. (2001). Inter-biome comparison of factors controlling stream metabolism. *Freshwater Biology*, 46(11), 1503–1517. <https://doi.org/10.1046/j.1365-2427.2001.00773.x>
- Odum, H. T. (1956). Primary production in flowing waters. *Limnology & Oceanography*, 1(2), 102–117. <https://doi.org/10.4319/llo.1956.1.2.0102>
- Palumbo, J. E., & Brown, L. C. (2014). Assessing the performance of reaeration prediction equations. *Journal of Environmental Engineering*, 140(3), 04013013. [https://doi.org/10.1061/\(asce\)ee.1943-7870.0000799](https://doi.org/10.1061/(asce)ee.1943-7870.0000799)
- Pathak, D. (2022). MUFT model. Zenodo. <https://doi.org/10.5281/zenodo.7197544>
- Pathak, D., Hutchins, M., Brown, L. E., Loewenthal, M., Scarlett, P., Armstrong, L., et al. (2022). High-resolution water-quality and ecosystem-metabolism modeling in lowland rivers. *Limnology & Oceanography*, 67(6), 1313–1327. <https://doi.org/10.1002/lno.12079>
- Payn, R. A., Hall, R., Jr., Kennedy, T. A., Poole, G. C., & Marshall, L. A. (2017). A coupled metabolic-hydraulic model and calibration scheme for estimating whole-river metabolism during dynamic flow conditions. *Limnology and Oceanography: Methods*, 15(10), 847–866. <https://doi.org/10.1002/lom3.10204>
- Poff, N. L., & Zimmerman, J. K. (2010). Ecological responses to altered flow regimes: A literature review to inform the science and management of environmental flows. *Freshwater Biology*, 55(1), 194–205. <https://doi.org/10.1111/j.1365-2427.2009.02272.x>
- Pulg, U., Stranzl, S., Vollset, K. W., Barlaup, B. T., Olsen, E., Skår, B., & Velle, G. (2016). *Gassmetning i Otra nedenfor Brokke kraftverk (Tech. Rep. No. 1892-8889)*. NORCE Norwegian Research Centre AS.
- Raymond, P. A., Hartmann, J., Lauerwald, R., Sobek, S., McDonald, C., Hoover, M., et al. (2013). Global carbon dioxide emissions from inland waters. *Nature*, 503(7476), 355–359. <https://doi.org/10.1038/nature12760>
- Raymond, P. A., Zappa, C. J., Butman, D., Bott, T. L., Potter, J., Mulholland, P., et al. (2012). Scaling the gas transfer velocity and hydraulic geometry in streams and small rivers. *Limnology and Oceanography: Fluids and Environments*, 2(1), 41–53. <https://doi.org/10.1215/21573689-1597669>
- Rørslett, B. (1988). Aquatic weed problems in a hydroelectric river: The R. Otra, Norway. *Regulated Rivers: Research & Management*, 2(1), 25–37. <https://doi.org/10.1002/rrr.3450020104>
- Runkel, R. L. (1998). One-dimensional transport with inflow and storage (OTIS). In *A solute transport model for streams and rivers* (Vol. 98). U.S. Department of the Interior, US Geological Survey.
- Santos Santos, T. F., & Camacho, L. A. (2022). An integrated water quality model to support multiscale decisions in a highly altered catchment. *Water*, 14(3), 374. <https://doi.org/10.3390/w14030374>
- Segatto, P. L., Battin, T. J., & Bertuzzo, E. (2020). Modeling the coupled dynamics of stream metabolism and microbial biomass. *Limnology & Oceanography*, 65(7), 1573–1593. <https://doi.org/10.1002/lno.11407>
- Segatto, P. L., Battin, T. J., & Bertuzzo, E. (2021). The metabolic regimes at the scale of an entire stream network unveiled through sensor data and machine learning. *Ecosystems*, 24(7), 1–18. <https://doi.org/10.1007/s10021-021-00618-8>
- Sincock, A. M. (2002). *Conceptual river water quality modeling under dynamic conditions (Unpublished doctoral dissertation)*. Imperial College London.
- Sincock, A. M., & Lees, M. (2002). Extension of the quasar river-water quality model to unsteady flow conditions. *Water and Environment Journal*, 16(1), 12–17. <https://doi.org/10.1111/j.1747-6593.2002.tb00361.x>
- Sincock, A. M., Wheeler, H. S., & Whitehead, P. G. (2003). Calibration and sensitivity analysis of a river water quality model under unsteady flow conditions. *Journal of Hydrology*, 277(3–4), 214–229. [https://doi.org/10.1016/s0022-1694\(03\)00127-6](https://doi.org/10.1016/s0022-1694(03)00127-6)
- Song, C., Dodds, W. K., Rüegg, J., Argerich, A., Baker, C. L., Bowden, W. B., et al. (2018). Continental-scale decrease in net primary productivity in streams due to climate warming. *Nature Geoscience*, 11(6), 415–420. <https://doi.org/10.1038/s41561-018-0125-5>
- Spear, R. C., & Hornberger, G. (1980). Eutrophication in peel inlet—II. Identification of critical uncertainties via generalized sensitivity analysis. *Water Research*, 14(1), 43–49. [https://doi.org/10.1016/0043-1354\(80\)90040-8](https://doi.org/10.1016/0043-1354(80)90040-8)
- Standing Committee of Analysts. (1989). Five days biochemical oxygen demand (BOD5) (Tech. Rep.).
- Streeter, H., & Phelps, E. B. (1925). *A study of the pollution and natural purification of the Ohio River. III. Factors concerned in the phenomena of oxidation and reaeration (Tech. Rep. No. 146)*. United States Public Health Service.
- Uehlinger, U., Kawecka, B., & Robinson, C. (2003). Effects of experimental floods on periphyton and stream metabolism below a high dam in the Swiss Alps (River Spöl). *Aquatic Sciences*, 65(3), 199–209. <https://doi.org/10.1007/s00027-003-0664-7>
- Vandenbergh, V., Van Griensven, A., & Bauwens, W. (2001). Sensitivity analysis and calibration of the parameters of ESWAT: Application to the River Dender. *Water Science and Technology*, 43(7), 295–301. <https://doi.org/10.2166/wst.2001.0438>
- Venables, W., & Ripley, B. (2002). *Modern applied statistics with S* (4th ed.). Springer.
- Von Schiller, D., Acuña, V., Aristi, I., Arroita, M., Basaguren, A., Bellin, A., et al. (2017). River ecosystem processes: A synthesis of approaches, criteria of use and sensitivity to environmental stressors. *Science of the Total Environment*, 596, 465–480. <https://doi.org/10.1016/j.scitotenv.2017.04.081>
- Wagner, R. J., Boulger, R. W., Jr., Oblinger, C. J., & Smith, B. A. (2006). Guidelines and standard procedures for continuous water-quality monitors: Station operation, record computation, and data reporting (Tech. Rep.).

- Wallis, S. G., & Manson, J. R. (2018). Flow dependence of the parameters of the transient storage model. In *Free surface flows and transport processes* (pp. 477–488). Springer.
- Wallis, S. G., Young, P., & Beven, K. (1989). Experimental investigation of the aggregated dead zone model for longitudinal solute transport in stream channels. *Proceedings - Institution of Civil Engineers*, 87(1), 1–22. <https://doi.org/10.1680/iicep.1989.1450>
- Waylett, A., Hutchins, M., Johnson, A., Bowes, M., & Loewenthal, M. (2013). Physico-chemical factors alone cannot simulate phytoplankton behavior in a lowland river. *Journal of Hydrology*, 497, 223–233. <https://doi.org/10.1016/j.jhydrol.2013.05.027>
- Webster, J. R., Mulholland, P. J., Tank, J. L., Valett, H. M., Dodds, W. K., Peterson, B. J., et al. (2003). Factors affecting ammonium uptake in streams—An inter-biome perspective. *Freshwater Biology*, 48(8), 1329–1352. <https://doi.org/10.1046/j.1365-2427.2003.01094.x>
- Weiss, R. F. (1970). The solubility of nitrogen, oxygen, and argon in water and seawater. *Deep Sea Research and Oceanographic Abstracts*, 17(4), 721–735. [https://doi.org/10.1016/0011-7471\(70\)90037-9](https://doi.org/10.1016/0011-7471(70)90037-9)
- Whitehead, P., Williams, R., & Lewis, D. (1997). Quality simulation along river systems (QUASAR): Model theory and development. *Science of the Total Environment*, 194, 447–456. [https://doi.org/10.1016/s0048-9697\(96\)05382-x](https://doi.org/10.1016/s0048-9697(96)05382-x)
- Wright, R. F., Couture, R.-M., Christiansen, A. B., Guerrero, J.-L., Kaste, Ø., & Barlaup, B. T. (2017). Effects of multiple stresses hydropower, acid deposition and climate change on water chemistry and salmon populations in the River Otra, Norway. *Science of the Total Environment*, 574, 128–138. <https://doi.org/10.1016/j.scitotenv.2016.09.044>
- Yang, H., Andersen, T., Dörsch, P., Tominaga, K., Thrane, J.-E., & Hessen, D. O. (2015). Greenhouse gas metabolism in Nordic boreal lakes. *Biogeochemistry*, 126(1), 211–225. <https://doi.org/10.1007/s10533-015-0154-8>
- Ye, S., Covino, T. P., Sivapalan, M., Basu, N. B., Li, H.-Y., & Wang, S.-W. (2012). Dissolved nutrient retention dynamics in river networks: A modeling investigation of transient flows and scale effects. *Water Resources Research*, 48(6). <https://doi.org/10.1029/2011wr010508>
- Young, R. G., Matthaei, C. D., & Townsend, C. R. (2008). Organic matter breakdown and ecosystem metabolism: Functional indicators for assessing river ecosystem health. *Journal of the North American Benthological Society*, 27(3), 605–625. <https://doi.org/10.1899/07-121.1>
- Zimmerman, J. K., Letcher, B. H., Nislow, K. H., Lutz, K. A., & Magilligan, F. J. (2010). Determining the effects of dams on subdaily variation in river flows at a whole-basin scale. *River Research and Applications*, 26(10), 1246–1260. <https://doi.org/10.1002/rra.1324>

## References From the Supporting Information

- Poole, G., O'daniel, S., Jones, K., Woessner, W., Bernhardt, E., Helton, A., et al. (2008). Hydrologic spiraling: The role of multiple interactive flow paths in stream ecosystems. *River Research and Applications*, 24(7), 1018–1031. <https://doi.org/10.1002/rra.1099>
- Reichert, P., Uehlinger, U., & Acuña, V. (2009). Estimating stream metabolism from oxygen concentrations: Effect of spatial heterogeneity. *Journal of Geophysical Research: Biogeosciences*, 114(G3), G03016. <https://doi.org/10.1029/2008jg000917>